Clumped isotopes in near surface atmospheric CO_2 over land, coast and ocean in Taiwan and its vicinity

Amzad Hussain Laskar[1] and Mao-Chang Liang[1,2,3*]

[1]Research Center for Environmental Changes, Academia Sinica, Taipei, Taiwan

[2]Graduate Institute of Astronomy, National Central University, Taiwan

[3]Department of Physics, University of Houston, USA

Correspondence to: Mao-Chang Liang (mcl@rcec.sinica.edu.tw)

Abstract

Molecules containing two rare isotopes (e.g., $^{13}C^{18}O^{16}O$ in CO_2), called clumped isotopes, in atmospheric CO_2 are powerful tools to provide an alternative way to independently constrain the sources of CO_2 in the atmosphere because of their unique physical and chemical properties. We presented clumped isotope data (Δ_{47}) in near surface atmospheric CO_2 from urban, sub-urban, ocean, coast, high mountain (~3.2 km a.s.l.) and forest in Taiwan and its vicinity. The primary goal of the study was to use the unique Δ_{47} signature in air CO_2 to show the extents of its deviations from thermodynamic equilibrium due to different processes such as photosynthesis, respiration, local anthropogenic emissions, which the commonly used tracers such as $\delta^{13}C$ and $\delta^{18}O$ cannot provide. We also explored the potential of Δ_{47} to identify/quantify the contribution of CO_2 from various sources. Atmospheric CO_2 over ocean was found to be in thermodynamic equilibrium with the surrounding surface sea water. Respired CO_2 was also in close thermodynamic equilibrium at ambient air temperature. In contrast, photosynthetic activity result in significant deviation in Δ_{47} values from that expected thermodynamically. The disequilibrium could be a consequence of kinetic effects associated with the diffusion of CO_2 in and out of the leaf stomata. We observed that $\delta^{18}O$ and Δ_{47} do not vary similarly when photosynthesis was involved unlike simple water-CO_2 exchange. Additionally we obtained Δ_{47} values of car exhaust CO_2 that were significantly lower than the atmospheric CO_2 but higher than that expected at the combustion temperature. In urban and sub-urban regions, the Δ_{47} values were found to be lower than the thermodynamic equilibrium values at the ambient temperature, suggesting contributions from local combustion emissions.

Keywords: clumped isotopes; atmospheric CO_2; thermodynamic equilibrium; anthropogenic; car exhaust

1. Introduction

The budget of atmospheric CO_2 is widely studied using the temporal and spatial variations in concentration and conventional isotopic compositions ($\delta^{13}C$ and $\delta^{18}O$) of CO_2 (Francey and Tans, 1987; Francey et al., 1995; Yakir and Wang, 1996; Ciais et al., 1995a,b, 1997; Peylin et al., 1999; Cuntz et al., 2003; Drake et al., 2011; Welp et al., 2011; Affek and Yakir., 2014). $\delta^{13}C$ is useful to differentiate the exchange of CO_2 with the ocean and land-biospheres. This is due to the fact that the photosynthetic discrimination against ^{13}C during exchange with land plants is higher than that associated with the chemical dissolution of CO_2 in the ocean (e.g., Tans et al., 1993; Ciais et al., 1995a; Francey et al., 1995; Ito, 2003; Bowling et al., 2014). The major limitation of $\delta^{13}C$ is that it cannot distinguish CO_2 produced by high temperature combustion or low temperature respiration (Affek and Eiler, 2006; Laskar et al., 2016a). $\delta^{18}O$ in atmospheric CO_2 is mainly controlled by various water reservoirs (ocean, leaf and soil). In urban locations, a significant fraction of CO_2 may have combustion origin possessing $\delta^{18}O$ signature of atmospheric O_2 (Kroopnick and Craig, 1972; Ciais et al., 1997; Yakir and Wang, 1996). $\delta^{18}O$ is used for partitioning net CO_2 terrestrial fluxes between soil respiration and that exchange with plant leaves, the exchange rate is enhanced by the presence of carbonic anhydrase in plants and soils (Francey and Tans, 1987; Farquhar and Lioyd, 1993; Yakir and Wang, 1996; Ciais et al., 1997; Peylin et al., 1999; Murayama et al., 2010; Welp et al., 2011). This is because $\delta^{18}O$ of CO_2 fluxes originated from soil respiration are different from that exchanged with leaf water. $\delta^{18}O$ in soil water reflect the $\delta^{18}O$ value of local meteoric water while leaf water is relatively enriched due to transpiration. The $\delta^{18}O$ values from these processes and interactions are different and hence the tracer is widely used for constraining the gross production of CO_2 (Francey and Tans, 1987; Ciais et al., 1997; Gillon and Yakir, 2001; Cuntz et al., 2003; Welp et al., 2011). However, due to rapid exchange of oxygen isotopes between CO_2 and different water reservoirs with diverse $\delta^{18}O$ and processes such as evapotranspiration complicate its interpretation (Riley et al., 2003).

The doubly substituted isotopologues or clumped isotopes such as $^{13}C^{18}O^{16}O$ in CO_2, denoted by Δ_{47}, provides an additional and independent constraint to study the atmospheric CO_2 budget. Δ_{47} in air CO_2 can help to identify the mechanisms for CO_2 production and consumption. Unlike conventional isotopes, clumped isotope studies for the atmospheric CO_2 are very limited mainly because of challenges to apply it to the atmospheric study (Eiler and Schauble, 2004; Affek et al., 2007; Yeung et al., 2009). The available data are not sufficient

to address some key issues such as quantification of CO_2 from different sources and to what extent the air CO_2 is in thermodynamic equilibrium with leaf and surface waters, especially in regions with strong anthropogenic activities such as urban areas. Also the effect of photosynthesis on the Δ_{47} of air CO_2 has not been studied rigorously. $\delta^{18}O$ and Δ_{47} were reported to have similar time-scales for the isotope exchange between CO_2 and water (Affek, 2013; Clog et al., 2015), but no comparative study on their behavior in presence of other processes such as photosynthesis and respiration was done. A combined assessment from all the three aforementioned isotopic tracers can better constrain the budget of CO_2 and associated processes than $\delta^{13}C$ or $\delta^{18}O$ alone.

Theoretically it is shown that in thermodynamic equilibrium, Δ_{47} values of CO_2 are temperature dependent (Eiler and Schauble, 2004; Wang et al., 2004), verified over a wide range from 10 to 1000 ^{o}C (Dennis et al., 2011). Processes that involve CO_2 and liquid water as medium, such as isotopic exchange with ocean water are expected to have Δ_{47} values close to the thermodynamic equilibrium. Δ_{47} values in ambient air CO_2 should reflect a balance of CO_2 fluxes between biosphere-atmosphere exchange, ocean-atmosphere exchange, and emissions from combustion sources. Photosynthesis involves gas phase diffusion of CO_2 into leaves, fixes ~1/3 of the CO_2, and returns the rest back to the atmosphere. CO_2 molecules inside a leaf are generally expected to be in thermodynamic equilibrium with leaf water because of presence of enzymatic carbonic anhydrase that greatly enhances the isotopic exchange (Cernusak et al., 2004). Δ_{47} values of soil respired CO_2 is also not well constrained, though it is believed to be in thermodynamic equilibrium with the soil water (Eiler and Schauble, 2004).

Here, we present clumped and conventional isotope data in near surface air CO_2 covering a wide variety of processes and interactions. Air samplings were made in South China Sea, two coastal stations in northern Taiwan, an urban traffic street, a sub-urban location, a forest site, a greenhouse, top of a high mountain and car exhausts. The study was designed and aimed to show the extents of the deviations of near surface atmospheric CO_2 from thermodynamic equilibrium with local surface water. Possible influences from other processes such as anthropogenic emission, respiration, and photosynthesis on clumped isotopes were explored.

2. Materials and methods

Stable isotopic compositions of CO_2 including mass 47 were measured using a Finnigan MAT 253 gas source stable isotope ratio mass spectrometer configured to measure ion beams corresponding to M/Z 44 through 49. The instrument registers the major ion beams (44, 45 and 46) through resistors 10^8, 3×10^{10}, and 10^{11} Ohm, respectively, and minor ion beams (47, 48 and 49) through 10^{12} Ohm. All the measurements were carried out at Research Center for Environmental Changes, Academia Sinica, Taiwan.

Air samples were collected in 2 L flasks and compressed to 2 atmospheric pressure using a membrane pump. The flasks, equipped with two stopcocks, were first flushed with the ambient air for ~10 mins before starting the sample collection. We then closed the downstream end stopcock, allowed the pressure to build to 2 atm and then isolated by closing the other stopcock. The air pumping for flushing and sampling was carried out through a column packed with magnesium perchlorates to remove moisture. The moisture content was reduced from the ambient value of 70-90 % to less than 1 % relative humidity, checked using a LI-COR infrared gas analyzer (model 840A, LI-COR, USA). See, for example, Liang and Mahata (2015) for more details of air sampling.

To show how photosynthesis and respiration affect the abundances of CO_2 isotopologues and to demonstrate what different information the Δ_{47} can give from the other isotopologues, we performed analyses for CO_2 collected in a controlled greenhouse with cemented floor located in the top (3^{rd}) floor of the Greenhouse Building, Academia Sinica. The size of the greenhouse was about 8m long, 5m wide and 5m high. It was closed at least one day before each experiment and the ventilation was kept off. More than 70 % of the ground area inside the greenhouse was occupied with *Cinnamomum cassia* plants, each of ~2 m height kept in pots. Samples were collected at intervals of less than half an hour to a few hours on three sunny days and one cloudy day to investigate the influence of photosynthesis and respiration on the isotopologues of CO_2. Inside the room relative humidity was ~50-70 % for the three sunny days and was above 90 % for the cloudy day.

Forest air CO_2 was collected from a dense natural forest at the west end of the Academia Sinica Campus. The vegetation mainly consists of medium to big size trees with canopy heights varying between 10 to 20 m. The samples were collected ~100 m inside the forest on a small plateau at a height of ~30 m from the ground in the slope of a hill; the dense

vegetation allowed little sunlight penetrating to the surface. The relative humidity at the site was 80-90 % during the sampling days and wind speed was nearly zero due to presence of hills on three sides of the sampling spot. Marine air was collected during a cruise in the South China Sea (for the cruise track see Figure 1) at a height of ~10 m a.s.l. and from two coastal stations: Keelung (25°09′6″ N, 121°46′22″ E) and Fuguei Cape (25°18′ N, 121°32′ E) (Figure 1) at a height of ~5 m and ~20 m a.s.l. respectively. Sea surface temperatures were measured at the time of sampling. Urban air was collected at a bus stop on Roosevelt Road, a busy street in Taipei. Sub-urban air was collected from an open roof (~30 m above ground) of Institute of Earth Science Building, Academia Sinica (AS; 25°2′41″ N, 121°36′52″ E); grassland air was collected from a grass field in front of the Department of Atmospheric Science, National Taiwan University Campus (NTU; 25° 1′ N, 121°30′ E), Taipei. In addition, we collected air from the summit of the Hehuan mountain (24°8′15″ N, 121°16′32″ E, 3.2 km a.s.l.) (Figure 1) on 9th October, 2013. All air samplings were made when there was no rain to avoid direct interaction with the rainwater. Car exhausts were collected from a Mazda 3000cc TRIBUTE and a Mitsubishi 2400cc New Outlander, using evacuated 2L glass flasks from ~20 cm inside the exhaust pipes through a column of magnesium perchlorate.

CO_2 was extracted from air using a glass vacuum line connected to a turbo molecular pump by cryogenic technique. The vacuum line as well as the sample flask connection assembly including its head space was pumped to high vacuum before starting the CO_2 extraction. Air in the flask was pumped through a series of five coiled traps, with the first two immersed in dry ice-acetone slush (-77 °C) for trace moisture removal followed by three in liquid nitrogen (-196 °C). CO_2 was collected from the traps immersed in liquid nitrogen by repeated freeze-thaw technique at liquid nitrogen and dry ice temperatures for further removal of traces of water (see Mahata et al., 2012 and Liang and Mahata, 2015 for details). The air was pumped for 40-45 minutes at a controlled rate of ~90 mL/min using a mass flow controller; the pressure on the post mass flow controller was ~10 mm of Hg. No measurable isotopic fractionation caused by mass flow controller at this flow rate was observed, checked using several aliquots of air from a high volume compressed air cylinder (~40 L at 2000 psi). For car exhaust, an aliquot of exhaust air was transferred to a 60 mL bottle and CO_2 was fully

extracted cryogenically following the same protocol as discussed above (but with mass flow controller step skipped).

CO_2 was further purified from other condensable species like N_2O, CH_4, and hydrocarbons by means of gas chromatography (Agilent 6890N, with a 3.0 m × 0.3 cm stainless steel column packed with PorapakQ 80/100 mesh, supplied by Supelco Analytical, Bellefonte, PA, USA) with the column kept at -10 ^oC. High purity helium (>99.9999 % supplied by Air Products and Chemicals, Inc.) at 20 mL/min was used as carrier gas. CO_2 was eluted first, followed forthwith by N_2O, and CH_4, hydrocarbons and traces of water came out much later. To get an optimized condition for CO_2, we checked the separation of CO_2 from N_2O with varying proportions and at various temperatures (25 ^oC to -20 ^oC) and found a temperature of -10 ^oC at which column separated CO_2 from N_2O perfectly (see Laskar et al., 2016b for details). The column was baked at 200 ^oC for more than 2 hours prior to use. The conditioned column is good for purifying three samples. At the end of the day, long baking (8-10 hours) was performed. At the initial phase the working gas was taken from a high purity commercial CO_2 called AS-2 ($\delta^{13}C$ = -32.54 ‰ with respect to VPDB and $\delta^{18}O$ = 36.61 ‰ with respect to VSMOW) procured from a local supplier (Air Products and Chemicals, Inc.). As the difference between the isotopic compositions of samples and AS-2 was high, we later changed the reference to Oztech CO_2 ($\delta^{13}C$ = -3.59‰ and $\delta^{18}O$ = 24.96 ‰) (Oztech Trading Corporation, USA) from December 2014 onward. No detectable difference in isotopic compositions including Δ_{47} was observed between the analyses from different working references. All $\delta^{13}C$ values presented in this work are expressed in VPDB scale and $\delta^{18}O$ in VSMOW scale, unless specified otherwise. Δ_{47} is calculated following (Affek and Eiler, 2006):

$$\Delta_{47}=\left[\frac{R^{47}}{2R^{13}R^{18}+2R^{17}R^{18}+R^{13}\left(R^{17}\right)^2}-\frac{R^{46}}{2R^{18}+2R^{13}R^{17}+\left(R^{17}\right)^2}-\frac{R^{45}}{R^{13}+2R^{17}}+1\right]\times 1000 \quad (1)$$

where R^{13} and R^{18} (ratios $^{13}C/^{12}C$ and $^{18}O/^{16}O$) are obtained by measuring the conventional masses 44, 45 and 46 in the same CO_2 sample and R^{17} is calculated assuming a mass dependent relation with R^{18} given by $R^{17}=R^{17}{}_{VSMOW}\left(R^{18}/R^{18}{}_{VSMOW}\right)^{\lambda}$, where exponent λ=0.5164 is used for all Δ_{47} calculations (Affek and Eiler, 2006). The value of λ varies between 0.516 and 0.523 (Hoag et al., 2005; Barkan and Luz, 2012; Hoffmann et al., 2012; Thiemens et al., 2014). The variation in Δ_{47} was less than 0.01 ‰ at 25 ^oC when the exponent

was varied over the aforementioned range. This variation was comparable to the measurement uncertainty and hence not considered here; all the calculations were based on λ=0.5164. Δ_{47} is obtained by measuring CO_2 with respect to which the isotopes among various CO_2 isotopologues are distributed randomly (Δ_{47} ~ 0 ‰). Practically, this random distribution is approached by heating CO_2 at 1000 ^{o}C for more than two hours (Eiler and Schauble, 2004; Affek and Eiler, 2006). Measurements were made with a stable ~12 volt signal at mass 44, with peak centring, background scanning, and pressure-balancing before each acquisition started. Each sample was analyzed for 10 acquisitions, 10 cycles each at an integration time of 8 s; the total analysis time was approximately 2.5 h. Masses 48 and 49 were monitored to check isobaric interferences due to contamination of hydrocarbons (Ghosh et al., 2006). Details about the corrections due to nonlinearity related to Δ_{47} measurements in the mass spectrometer, reference frame equation for expressing the measured Δ_{47} values in absolute reference frame (ARF) were discussed in Laskar et al. (2016b). To obtain the temperature from the Δ_{47} values, we used the following relation (Dennis et al., 2011):

$$\Delta_{47} = 0.003\left(\frac{1000}{T}\right)^4 - 0.0438\left(\frac{1000}{T}\right)^3 + 0.2553\left(\frac{1000}{T}\right)^2 - 0.2195\left(\frac{1000}{T}\right) + 0.0616 \quad (2)$$

The reproducibility (1-σ standard deviation) for air CO_2 measurements was established from three aliquots of CO_2 extracted from a compressed air cylinder with CO_2 concentration ([CO_2]) of ~388 ppmv. The 1-σ standard deviations were 0.07, 0.08, and 0.01 ‰ for $\delta^{13}C$, $\delta^{18}O$, and Δ_{47}, respectively (Table S1 in Supplement). The long-term reproducibility in Δ_{47} measurements was found to be 0.014 ‰ (Laskar et al., 2016b) and the accuracy in Δ_{47} values in terms of temperature, based on CO_2 equilibrated with water at known temperatures were better than 3 ^{o}C (see Table S2 in Supplement).

For [CO_2] measurements, flasks of volume 350 cc were used. These small flasks were connected in series with the larger flasks used for isotopic measurements. [CO_2] was measured using a LI-COR infrared gas analyzer (model 840A, LI-COR, USA) at 4 Hz, smoothed with 20-s moving average. The analyzer was calibrated against a working standard (air compressed in a cylinder) with a nominal [CO_2] of 387.7 ppmv and a CO_2 free N_2 cylinder. The reproducibility of LI-COR was better than 1 ppmv. The working standard was calibrated using a commercial Picarro analyzer (model G1301, Picarro, USA) by a series of NOAA/GMD certified tertiary standards with [CO_2] of 369.9, 392.0, 409.2, and 516.3 ppmv,

with a precision (1-σ standard deviation) of 0.2 ppmv. The [CO_2] in car exhausts were estimated by gravimetric technique using an MKS Baratron gauge.

Ambient temperatures were taken from the nearest governmental weather stations (operated by Central Weather Bureau, Taiwan): Nankang (for AS; station code: C0A9G0; 25°03′27″ N, 121°35′41″ E, 42 m a.s.l.), Taipei (for NTU; station code: C1A730; 25°00' 58″ N, 121°31' 53″ E; 22 m a.s.l.), Hehuan mountain (station code: C0H9C1; 24°08′41″ N, 121°15′ 51″ E, 3240 m a.s.l.), and Keelung coast (for the two coastal sites; station code: 466940; 25°08′05″ N, 121°43′56″ E, 26.7 m a.s.l.).

3. Results

3.1 Greenhouse CO_2

Diurnal variation in the concentration and isotopic compositions of CO_2 inside the controlled greenhouse is shown in Figure 2. The lowest CO_2 concentration [CO_2] and highest $\delta^{13}C$ and $\delta^{18}O$ values were observed during late morning hours while highest [CO_2] and lowest $\delta^{13}C$ and $\delta^{18}O$ values were observed during night time and early morning before sunrise (Table 1 and Figure 2A-2C), indicating that respiration and photosynthesis played the major role in controlling the variations of the [CO_2] and isotopic compositions. Keeling plot, a graphical approach plotted between isotopic composition and the inverse of the concentration is used to determine the isotopic composition of the source (Pataki et al., 2003). It is valid for a mixing of two components; the intercept of the plot gives the source isotopic composition. Respiration was the main source of CO_2 here added to the background CO_2. Keeling analysis for $\delta^{13}C$ had an intercept of -26.32±0.40 ‰ (Figure 2D), a value expected for C_3 plant respired CO_2. The Keeling plot for $\delta^{18}O$ had an intercept of 30.68±0.73 ‰ (Figure 2E), which could be explained by a combined effect of respired CO_2 equilibrated with soil water and kinetic fractionation associated with the diffusion of CO_2 from soil to the air. A Keeling plot for $\delta^{13}C$ with the early morning and night time greenhouse data, when photosynthesis was absent, was found to have same intercept as observed with all the data, only the correlation was better for the latter (R^2=0.999, not shown). The tight correlations among [CO_2], $\delta^{13}C$ and

$\delta^{18}O$ (Figure 2D-2F) suggest that photosynthesis and respiration were the dominant processes controlling their variations while mixing with ambient air and anthropogenic contribution of CO_2 were insignificant.

In contrast, Δ_{47} shows different patterns of diurnal variability due to the effect of photosynthesis and respiration. Figures 3A-3D detail diurnal variations in Δ_{47} in the greenhouse CO_2 in four different days. The first three were bright sunny days with photosynthesis as the dominant process while the last one was a dark cloudy day affected more by respiration. To further reduce photosynthetic activity on the last day, two layers of black cloth that cut down the incident sunlight by ~50% were deployed. The measured Δ_{47} values were also compared with the thermodynamic equilibrium values. The maximum value of Δ_{47} was observed in the morning before ~8 AM and at night and the values were similar to the thermodynamic equilibrium values at the ambient temperatures. This indicates that the respired CO_2 was in close thermodynamic equilibrium with the leaf and soil water. The daytime (from 9 AM to 5 PM) Δ_{47} values, for the three sunny days were higher than the thermodynamic equilibrium values. The Δ_{47} values were observed to decrease steadily in the early morning before ~9 AM and increased afterwards (Figure 3). By comparing the Δ_{47} values acquired in the sunny days with that in the cloudy day, we noticed that when photosynthesis was weak, the Δ_{47} value was close to the thermodynamic equilibrium with soil and leaf water (Figure 4). The correlation between Δ_{47} and $[CO_2]$, $\delta^{13}C$ or $\delta^{18}O$ (Figure 3D) was observed only when the photosynthesis was weak. This suggests that Δ_{47} carries information different from concentration and conventional isotopic composition when photosynthesis occurs. See Section 4.1 for detailed discussion.

3.2 Car exhaust

The $[CO_2]$, $\delta^{13}C$ and $\delta^{18}O$ values of car exhaust CO_2 were 39350±50 ppmv, -27.70±0.03 ‰ and 25.35±0.07 ‰, respectively (Table 2). $\delta^{13}C$ value was similar to that reported elsewhere (Newman et al., 2008; Popa et al., 2014), the $\delta^{18}O$ was slightly higher than the atmospheric O_2 (~23.5 ‰), the source of O_2 for combustion. The average value of Δ_{47} for the exhausts from the two cars was 0.273±0.021 ‰, which gave a temperature of 282±17 ^{o}C (Table 2). This temperature is much higher than the fuel combustion temperatures (>800 ^{o}C). The possible reason for higher values of $\delta^{18}O$ and Δ_{47} in the exhaust CO_2 than expected was post

combustion partial exchange with water and other gaseous species, released during combustion, inside the catalytic converter and the exhaust pipe (see discussion in Sec. 4.2).

3.3 Atmospheric CO_2 over ocean and coasts

Isotopic compositions including Δ_{47} values obtained for CO_2 over ocean and coasts are presented in Table 3. The averaged [CO_2] over ocean between latitudes 18°03′ N and 21°17′ N was 395±7 ppmv, and the values of $\delta^{13}C$ and $\delta^{18}O$ were -8.43±0.19 ‰ and 40.72±0.20 ‰, respectively (Table 3). In the coastal stations, the averaged values of [CO_2], $\delta^{13}C$, and $\delta^{18}O$ were 397±10 ppmv, -8.48±0.11 ‰, and 40.70±0.29 ‰, respectively. Both the [CO_2] and $\delta^{13}C$ values over the ocean and coasts were similar to those observed at Mauna Loa during the sampling period, suggesting little contribution from local/regional anthropogenic sources. The Keeling analysis for $\delta^{13}C$ gave in intercept of -13.61 ‰ (Figure 5A) for the air CO_2 collected over the ocean and coasts. $\delta^{18}O$ of air CO_2 over the ocean were close to the isotopic equilibrium values with the surface sea water at the sea surface temperatures (see Sec 4.3). The Δ_{47} values varied between 0.880 ‰ and 0.946 ‰ for the marine and coastal CO_2 (Table 3, Figures 5B), similar to that predicted at thermodynamic equilibrium at sea surface temperatures (obtained using Eq. (2)). Therefore, both $\delta^{18}O$ and Δ_{47} values suggest that the air CO_2 over the ocean was in close thermodynamic equilibrium with the underlying sea water.

3.4 Atmospheric CO_2 over land

To show how anthropogenic emission affects the isotopic composition especially the Δ_{47} values, we analyzed atmospheric CO_2 samples collected near Roosevelt Road, a busy street in downtown Taipei. The averaged values of [CO_2], $\delta^{13}C$ and $\delta^{18}O$ obtained were 500±50 ppmv, -11.05±0.90 ‰, and 39.32±0.94 ‰, respectively (Table 4). A significantly higher [CO_2] and lower $\delta^{13}C$, and $\delta^{18}O$ values compared to the marine CO_2 showed signatures of a significant contribution from vehicular emissions. Δ_{47} values near Roosevelt Road were found to be in the range of 0.754‰ to 0.833 ‰, with an average of 0.807±0.028 ‰ (Table 4). The values were lower by ~0.15 ‰ compared to the thermodynamic equilibrium value at 20 °C, the

ambient temperature around the sampling time, indicating a significant fraction of CO_2 produced at higher temperatures, i.e., of combustion origin.

In the sub-urban location (Academia Sinica Campus), [CO_2] averaged over four months was 410±10 ppmv (Table 4), which was ~15 ppmv higher than that observed over the South China Sea and that at Mauna Loa Observatory during the time of sampling. The higher [CO_2] suggests contribution from local anthropogenic emissions. $\delta^{13}C$ values varied between -7.83 and -10.30 ‰, with an average of -8.78±0.50 ‰. Keeling analysis for $\delta^{13}C$ gave an intercept of -26.16±1.58 ‰ (Figure 6), indicating source of CO_2 from C_3 plant respiration and/or combustion. Δ_{47} values here varied between 0.853 ‰ and 0.972 ‰ (Table 4) with an average of 0.897±0.027 ‰, which were significantly less than the thermodynamic equilibrium values (assuming water bodies had the same temperature as the ambient) (Figure 7).

The averaged [CO_2], $\delta^{13}C$ and $\delta^{18}O$ over the grassland (inside National Taiwan University Campus) were 410±33 ppmv, -8.95±0.70 ‰ and 39.74±1.00 ‰, respectively. The Keeling plot for $\delta^{13}C$ gave an intercept of -16.98±1.02 ‰ (Figure 6), indicating that a significant fraction of CO_2 originated from C_4 vegetation. This is not surprising as the CO_2 was sampled over a C_4 dominated grassland (area: ~50 m x 50 m). Unlike greenhouse CO_2, no statistically significant correlation between $\delta^{18}O$ and 1/[CO_2] in air CO_2 in these sites was observed (not shown), probably due to influence of multiple sources and processes on oxygen isotopes of atmospheric CO_2. Figure 7C shows the Δ_{47} values in air CO_2 over the grassland at National Taiwan University Campus. A large variation in Δ_{47} was observed (0.885 - 0.989 ‰) with an average of 0.937±0.030 ‰. Some of the values were close to the thermodynamic equilibrium while the others deviated significantly.

In a small and dense forest near Academia Sinica Campus (Figure 1), average values of [CO_2], $\delta^{13}C$ and $\delta^{18}O$ in air CO_2 were 438±16 ppmv, -9.99±0.50 ‰ and 40.39±0.63 ‰, respectively (Table 4) during summer (Jul-Aug) of 2015. A significantly higher [CO_2] and lower $\delta^{13}C$ values than the background indicate strong contribution of CO_2 from local respiration. Δ_{47} values fall in the range of 0.887 ‰ to 0.920 ‰, with an average of 0.895±0.012 ‰ (Table 4). The values were similar to that expected at thermodynamic equilibrium (Figure 7D) except on 11th August, when a significant increase in Δ_{47} was observed. The deviation was probably due to influence of a super typhoon, which passed over the region on previous days mixing and transporting air masses regionally.

Over the top of the Hehuan mountain (~3.2 km a.s.l), $[CO_2]$, $\delta^{13}C$, and $\delta^{18}O$ values in air CO_2 samples collected on 9th October, 2013 were 364 ppmv, -8.23±0.02 ‰ and 40.59±0.30 ‰, respectively (Table 4). The lower $[CO_2]$ and higher $\delta^{13}C$ than Mauna Loa suggests photosynthetic uptake, which was also seen at grassland site and inside greenhouse on a few occasions. Here the averaged value of Δ_{47} was 0.904±0.009 ‰, slightly less than that expected at the ambient temperature (Table 4).

4. Discussion

A detailed discussion of the results obtained from different locations is presented below.

4.1 Greenhouse air CO_2

To minimize anthropogenic alteration and air mixing/transport and to maximize the variations of CO_2 isotopologues by biological processes, a controlled greenhouse provides an ideal environment. Diurnal variation was observed in $[CO_2]$, $\delta^{13}C$, $\delta^{18}O$ (Figure 2), and Δ_{47} (Figure 3) in the greenhouse. Good correlations between $[CO_2]$, $\delta^{13}C$ and $\delta^{18}O$ suggest common processes affecting all of them, and they were photosynthesis and respiration. Giving July 31st as an example, we estimated the rates of night-time respiration and daytime photosynthetic uptake using the conventional isotopic compositions (analysis of Δ_{47} is discussed separately below). The dimension of the greenhouse room was 8m, 5m and 5m (length, width and height). The night-time respiration rate was then estimated to be about ~10 ppmv per hour (considering change of $[CO_2]$ from 5:30 PM to 9:30 PM; Figure 2A), or ~4×10^{13} molecules cm^{-2} s^{-1}. Using simple isotopic mass balance, this increase of $[CO_2]$ could be satisfactorily explained assuming C_3 respiration as the main source of CO_2 ($\delta^{13}C \approx$ -26 ‰; intercept in Figure 2D) added to the background (-8.5 ‰). Similarly, the same conclusion could be derived by analyzing $\delta^{18}O$ considering $\delta^{18}O$ of respired and background CO_2 of 30.68 ‰ (intercept in Figure 2E) and ~40 ‰ respectively. Thus, we conclude that the main factor that affected the changes in concentration as well as the isotopic compositions in night-time was respiration.

The daytime net uptake rate can be estimated by taking the changes from early morning to noon time; the [CO_2] reduced by 110 ppmv, $\delta^{13}C$ increased by 3.46 ‰, and $\delta^{18}O$ by 2.23 ‰ in about six hours. We calculated the number of molecules and their changes inside the greenhouse assuming simple gas laws. The estimated net photosynthetic uptake was ~1×10^{14} molecules cm^{-2} s^{-1} assuming constant respiration rate that was observed in the night. The photosynthetic discrimination can be calculated using the Rayleigh distillation model

$$R = R_o f^{\alpha-1} \quad (3)$$

where R_o and R are the initial and modified $^{13}C/^{12}C$ or $^{18}O/^{16}O$ ratios (due to photosynthetic activity), respectively, f is the fraction of the material left, and α is the fractionation factor. The estimated discrimination in ^{13}C defined by (α-1), following equation (3), was -16.5 ‰, which was slightly higher than that expected for C_3 type vegetation (~ -20 ‰) (Farquhar et al., 1989). For ^{18}O, in addition to photosynthetic uptake, one has to consider an additional effect due to temperature-dependent water-CO_2 equilibrium fractionation. That is, the process decreases $\delta^{18}O$ by ~0.2 ‰ for an increase of 1 ^{o}C in temperature (Brenninkmeijer et al., 1983); from morning to noon time, the temperature effect reduced $\delta^{18}O$ by 4.4 ‰. Adding this factor to the observed change in $\delta^{18}O$ yielded a discrimination factor of -12.0 ‰; the value becomes -7.0 ‰, if this additional temperature-dependence is ignored. The value (-12.0 ‰) observed considering the additional exchange with the soil water was slightly higher than that observed previously (-14.4 ‰) (Flanagan et al., 1997). Here the $\delta^{13}C$ and $\delta^{18}O$ values of the respired components were assumed to be -26 ‰ and 30 ‰ respectively (see Sec. 3.1).

We assume that ca. 1/3 of the CO_2 molecules in stomata are fixed photosynthetically and the remaining retro-diffuse back to the atmosphere (Farquhar and Lloid, 1993) implying that the CO_2-water isotopic exchange rate was ~2×10^{14} molecules cm^{-2} s^{-1}. Also we assume that the CO_2 molecules that enter into the leaf stomata get isotopically equilibrated with the leaf water before diffusing back to the atmosphere. This implies an approximately 8 hours of oxygen isotope exchange time for CO_2 in the greenhouse room. As a result, we do not expect that CO_2 reached to complete isotopic equilibrium with the substrate water in a few hours inside the room. Δ_{47} values in the leftover CO_2 could be used to check the disequilibrium. The respired CO_2 were found to be in thermodynamic equilibrium at the ambient temperature, shown by the Δ_{47} values of CO_2 in the early morning and night-time (Figure 3A-3C) and that collected on a cloudy day with suppressed photosynthetic activity (Figure 3D). The close-thermodynamic equilibrium at reduced photosynthetic condition is also shown in Figure 4A

that deviation in Δ_{47} from that expected at ambient temperature is small. On sunny days, the $[CO_2]$, $\delta^{13}C$, and $\delta^{18}O$ values change by 50-115 ppm, 2-4 ‰, and 1.1-2.2 ‰, respectively, in a time period of ~5 hours in the morning (Figure 2). Figure 3 shows that the Δ_{47} values retained the thermodynamic equilibrium values in the morning hours (until 9 AM) and then deviate from the thermodynamic equilibrium later of the day. The maximal reduction in the Δ_{47} values during these morning hours was ~0.05 ‰ (Figures 3A-3C) which is significant, as this value is much higher than the uncertainty of the measurements. An increase in Δ_{47} values after ~9 AM was observed. We attribute these changes in the Δ_{47} values of the residual CO_2 to photosynthesis as it is seen when photosynthesis is strong. Also we note that there was no significant correlation/anti-correlation between $\delta^{18}O$ and Δ_{47} when photosynthesis was strong (Figure 3A-3C), but became significant when the photosynthesis was weak (Figure 3D). Therefore, the plant photosynthesis decouples Δ_{47} and $\delta^{18}O$; in contrast to pure water-CO_2 isotopic exchange where the two behave similarly as far as isotopic equilibration is concerned (Affek, 2013; Clog et al. 2015).

Strong influence of photosynthesis on Δ_{47} was also reported by Eiler and Schauble *(*2004). They observed decrease in the Δ_{47} values of the residual CO_2 due to photosynthetic assimilation though the effect observed was different for different species. Here we observed a decrease in Δ_{47} value of the residual CO_2 initially (first 2 hours) due to photosynthesis similar to that observed by Eiler and Schauble (2004) but later it starts increasing in response to the photosynthesis. Photosynthesis as a source of disequilibrium was also shown recently by analyzing the clumped isotopes of O_2 (Yeung et al., 2015). Though enzymatic carbonic anhydrase catalyzes the water-CO_2 isotopic exchange toward equilibrium (Peltier et al., 1995; Cernusak et al., 2004) its activity varies. A large variation in the activity of carbonic anhydrase in different vegetation types (C_3, C_4) or within the same type was noted previously (see Gillon and Yakir, 2001 and references therein). Therefore, the reaction may be incomplete which is limited by the enzymatic activity inside leaves. Furthermore, a box modelling by Eiler and Schauble (2004) demonstrated that gas diffusion through leaf stomata during photosynthesis fractionates the remaining air CO_2 Δ_{47} value deviating it from the thermodynamic equilibrium set by leaf water. Mixing of more than one component can also cause change in Δ_{47} when $\delta^{13}C$ and $\delta^{18}O$ of the components are different (Affek and Eiler, 2006; Laskar et al., 2016a), but this can easily be ruled out as it was not observed when photosynthesis was not very strong (Figure 3D). More rigorous investigations with controlled

experiments using different plants with diverse carbonic anhydrase activities are needed to resolve the issue.

Considering the discrimination for $\delta^{13}C$, $\delta^{18}O$ and variation in the concentration it is possible to model the observed isotopic profile. Rayleigh model (Eq. 3) in terms of δ notation can approximately be written as $\delta=\delta_o+\varepsilon\times\ln(f)$, where δ_o is the initial δ value, f is the fraction of material left and ε is the enrichment factor. Figure 8A shows the concentration profiles for 31st Jul, 2015 inside the greenhouse. With the calculated discrimination factors (ε) of -16.5 ‰ and -12.0 ‰ for $\delta^{13}C$, $\delta^{18}O$, the modelled isotopic profiles along with actual data are shown in Figure (8B&8C). The model data are generated using Rayleigh fractionation relation. Assuming this relation valid for Δ_{47}, a discrimination factor of 0.065 ‰ due to photosynthesis was observed in the morning hours of 31st July, 2015. Figure (8C) shows the Δ_{47} profile for the same day along with the actual observed values. The observed data match well with the model plots. Unlike δs, Δ_{47} is not a linear quantity as discussed later, the discrimination factor calculated may slightly change when non-linearity is taken into account. With more data, probably at leaf level will allow to estimate the photosynthetic discrimination for Δ_{47}.

4.2 Car exhaust CO_2

Ideally, the Δ_{47} value of car exhaust CO_2 should reflect the temperature of fuel combustion inside the combustion chamber which is >800 ^oC. However, the temperature estimated from Δ_{47} was found to be 283±18 ^oC. It is likely that interaction of the sample CO_2 with the exhaust gases and water inside catalytic converter and exhaust pipe modified the Δ_{47} values. Catalytic converter which oxidizes CO and hydrocarbons to CO_2 probably reset the clumped signatures at relatively lower temperature. During combustion water-vapor is also released. We observed that the exhaust gas contained a large amount of water vapor, part of which got condensed on the exhaust pipe and the front part of the magnesium perchlorate column. Partial equilibration with the stream of the exhaust gas and water inside catalytic converter and the exhaust pipe was the likely cause for higher Δ_{47} values than that expected. This was also supported by the higher $\delta^{18}O$ values than atmospheric O_2, the source of O_2 for water and CO_2 here. Normally isotopes in CO_2 do not exchange with water vapor, but exchange may take place at higher temperature in presence of catalyst. Inside catalytic converter, exchange could take place on the surface of the catalyst at elevated temperatures of 200 – 400 ^oC

(Farrauto and Heck, 1999; Kašpar et al., 2003; Klingstedt et al., 2006). Affek and Eiler (2007) also observed elevated Δ_{47} values for car exhausts and estimated a temperature of CO_2 production to be ~200 ^{o}C. The temperature estimated here (283 ^{o}C) is significantly higher than that observed by Affek and Eiler (2007). Difference could be due to different car models and the variations in the temperatures of the catalytic converters from car to car.

4.3 Marine and coastal air CO_2

Carbon Keeling plot for marine and coastal air CO_2 gave an intercept of -13.61±1.14 ‰ (Figure 5A), the source signature. The South China Sea is net source of CO_2 to the atmosphere (Zhai et al., 2005). The CO_2 released over ocean is mainly originated from the remineralization of organic matter in the deeper ocean (Francois et al., 1993; Goericke and Fry, 1994). The $\delta^{13}C$ value of such organic matter ranges between -20 and -30 ‰ in the tropical to subtropical oceans, the intercept observed here (-13.6 ‰) is much higher than this range, though the associated uncertainty is high due to a small span of the samples. A possibility is that the remineralized CO_2 gets equilibrated with the dissolved inorganic carbon before releasing to the atmosphere. Again a complete equilibration of the CO_2 with the dissolved inorganic carbon would lead to a $\delta^{13}C$ value of released CO_2 to be -9 to -10 ‰ (Mook, 1986; Boutton, 1991; Zhang et al., 1995; Affek and Yakir, 2014), the observed value of the intercept (-13.6 ‰) was significantly less than this. Therefore, we conclude that the CO_2 produced in the deeper ocean is partially equilibrated with the dissolved inorganic carbon before releasing to the atmosphere.

The $\delta^{18}O$ values of the surface sea water in the South China Sea region in summer (July-September) and winter (December-February) were about -1.7 ‰ and -0.6 ‰ (Ye et al., 2014). The sea surface temperatures in the summer and winter are about 28 and 24 ^{o}C, and the equilibrated $\delta^{18}O$ values of the atmospheric CO_2 should be 38.9 ‰ and 40.7 ‰, respectively assuming fractionation factors at the respective temperatures (Brenninkmeijer et al., 1983). Our observed values lie in the range of 40.4 ‰ to 41.0 ‰ (Table 3), consistent with the isotopic equilibrium values with the surface water. Therefore, we conclude that oxygen isotopes in near surface air CO_2 over ocean are close to the isotopic equilibrium with the surface sea water. This conclusion was further supported by the observed Δ_{47} values which were found to be close to thermodynamic equilibrium with the underlying sea surface

water at the sea surface temperature (Figure 5B). This is due to the same water-CO_2 exchange time for the two species (Affek, 2013; Clog et al., 2015). Comparing this observation with the greenhouse data above, we conclude that $\delta^{18}O$ and Δ_{47} behave similarly when equilibrium is achieved by simple water-CO_2 exchange but respond differently when photosynthesis is the main governing factor. Though carbonic anhydrase are also present in the surface ocean and marine phytoplankton does photosynthesis, $\delta^{18}O$ and Δ_{47} in air CO_2 over the ocean show the values at thermodynamic equilibrium unlike greenhouse. The degree of deviation from thermodynamic equilibrium probably increases with the increase in photosynthetic activity. Normally photosynthesis by oceanic plants is much less compared to their terrestrial counterparts, the deviation from thermodynamic equilibrium by the oceanic photosynthesis, if present, is probably not detectable with the present measurement precision. Compared to $\delta^{18}O$, Δ_{47} is process sensitive and is not affected by the isotopic composition of substrate water. Given that the surface air temperature is better measured, we believe the clumped isotopes potentially provide good tracers for global carbon flux study involving CO_2, complementing the commonly used species like [CO_2], $\delta^{13}C$, and $\delta^{18}O$.

In the coastal stations, Δ_{47} values were similar to the thermodynamic equilibrium with the sea surface water at the temperature of ~27 ^{o}C (Figure 5B). The recoded air temperature during the sampling period over the coasts varied between 14 and 24 ^{o}C and was not reflected in the Δ_{47} values. We note that the samples were collected from two open spaces in the coasts where strong north and northeasterly winds overwhelmed, carrying air masses from the oceans towards the sampling locations (See Table S3 in Supplement). Therefore, we expect the major contribution was marine air with little influence from local processes, which could occasionally cause deviation from the thermodynamic equilibrium values.

4.4 Urban and sub-urban air CO_2

A significant fraction of anthropogenic CO_2 was present in the air CO_2 over the urban site, indicated by the [CO_2] as well as isotopic compositions including Δ_{47}. Anthropogenic contribution can be estimated following a two component mixing: $\delta = f_{anth}\times\delta_{anth}+(1-f_{anth})\times\delta_{bgd}$, where δ's can be $\delta^{13}C$ or $\delta^{18}O$ or Δ_{47} and f's, the corresponding weighting factor, and subscripts 'anth' and 'bgd' refer to anthropogenic and background, respectively. We take the 'anthropogenic' end member as the isotopic compositions of the car exhaust values

549 (Table 2) and 'background' end member as the values observed over the ocean (for $\delta^{13}C$ and
550 $\delta^{18}O$, Table 3) and thermodynamic equilibrium value at the mean ambient temperature of ~20
551 ^{o}C in December (0.95 ‰ for Δ_{47}) at the sampling site, respectively. Assuming that the excess
552 in [CO_2] above the background was originated from vehicular emissions, the values of the
553 $\delta^{13}C$, $\delta^{18}O$, and Δ_{47} in the urban site obtained using the mixing equation were -12.26 ‰,
554 37.68 ‰, and 0.809 ‰, respectively, which were similar to those observed (Table 4). Δ_{47} is
555 not a conserved quantity and a linear mixing is not valid when the $\delta^{13}C$ and $\delta^{18}O$ of the
556 components are widely different (Affek and Eiler, 2006; Laskar et al., 2016a). In the present
557 case, the isotopic compositions of the two components were not drastically different and
558 fraction of anthropogenic CO_2 was much less (<1/4) than the background CO_2, and hence the
559 error due to linear approximation was small (comparable to the uncertainty of measurement).
560 Anthropogenic CO_2 can also be quantified using radiocarbon (^{14}C) as fossil fuels are highly
561 depleted in ^{14}C (Miller et al., 2012); however, it cannot distinguish difference between CO_2
562 from two sources with modern carbon.

563 No systematic diurnal or temporal trend was observed in the Δ_{47} values in the sub-urban CO_2
564 during the sampling period (Figure 7B). However a weak trend was seen in $\delta^{13}C$ and $\delta^{18}O$
565 (not shown) in response to the seasonal variation of the carbon assimilation and oxygen
566 isotopes in the rainwater (Peng et al., 2010; Laskar et al., 2014). This furthermore
567 demonstrates that Δ_{47} behaves differently from [CO_2], $\delta^{13}C$, and $\delta^{18}O$. Almost all measured
568 Δ_{47} values were lower than that expected at the ambient temperature except two days: 9th
569 November, 2013 and 3rd February, 2014. $\delta^{13}C$ values were also slightly lower than the
570 background values. The reduced values of Δ_{47} could be due to contribution of CO_2 from
571 combustion processes which produced CO_2 with low Δ_{47} values as discussed in Section 4.2.
572 We estimated the contribution of local anthropogenic emissions in $\delta^{13}C$ and Δ_{47} using the two
573 components mixing discussed above. The components were the background air CO_2 and car
574 exhausts. The expected $\delta^{13}C$ and Δ_{47} values of the mixture were -9.1 ‰ and 0.92 ‰,
575 respectively. The observed Δ_{47} value was significantly different from that estimated from
576 simple two component mixing, though it was not different for $\delta^{13}C$. After subtracting the
577 local anthropogenic contribution from the observed Δ_{47} values, a difference of ~0.026 ‰
578 between the observed and estimated remains for sub-urban station and it disappeared for
579 urban station (see Table S4 in Supplement). This was not obvious in $\delta^{13}C$ probably due to
580 larger variation. The lower Δ_{47} values in sub-urban station could possibly be due to kinetic

effect during photosynthetic assimilation, partial contribution of marine air, or a combination of them. It could also be due to underestimation of the anthropogenic CO_2 at the sampling spot. The regional background [CO_2] here could be lower than that assumed and the actual anthropogenic fraction of CO_2 could be higher. The marine air in the vicinity of Taiwan, which was at thermodynamic equilibrium with the surface sea water as discussed earlier, might have contributed partially to the air CO_2 at the sampling site. Varying contribution of marine air could explain the lower Δ_{47} values to some extent. The most plausible cause for observed deviation in the Δ_{47} values that cannot be accounted for by anthropogenic and marine alterations was photosynthesis, as discussed earlier for greenhouse CO_2. This is not unreasonable, as the Academia Sinica Campus is surrounded by thick greeneries.

On 9th Nov, 2013 and 3rd February, 2014, the Δ_{47} values were close to that expected at thermodynamic equilibrium (Figure 7B). The Δ_{47} values on 9th November were not very different from the values reported for the previous or next days. However, the calculated thermodynamic equilibrium values on that day were relatively low due to high ambient temperatures; air CO_2 probably did not get enough time to equilibrate. On 3rd Febrauray, 2014, the Δ_{47} values were higher and comparable to the thermodynamic equilibrium values expected at ambient temperatures. A likely explanation is that the air on that day was a mixture of two components at the sampling region. A relatively strong wind from the southern land (Table S3 in Supplement) contributed the air CO_2 and the higher Δ_{47} values were probably due to mixing of the local air with that transported from the south of Taipei.

4.5 Grassland, forest and high mountain air CO_2

In the grassland station in Taipei city, the Keeling plot intercept for $\delta^{13}C$ **(**-17.0±1.0 ‰) (Figure 5D) indicated some sources of CO_2 with higher $\delta^{13}C$ values compared to the most expected sources, namely, C_3 vegetation and vehicle emission with a $\delta^{13}C$ value of ~ -27 ‰. Though the sampling station was located in an urban region, the sampling spot was at least ~150 m away from traffic streets, such as Keelung road, along with ~60 m wide, ~10 m high C_3 trees in between. As a result, anthropogenic signals were not very prominent. The samples were collected just above the surface of the grasses. Tropical warm grasses are mainly C_4 type with $\delta^{13}C$ in the range of -9 to -19 ‰ and a global average of -13 ‰ (Deines, 1980). We measured $\delta^{13}C$ values of a few grass samples and found values in the range of -15 to -17 ‰.

The soil and grass respired CO_2 with higher $\delta^{13}C$ contributed significantly to the near surface CO_2, resulting in a higher value of intercept (-17 ‰). The concentration was observed to be less than the background level sometimes, probably due to strong CO_2 uptake by plants. The temperature gradually decreased from 26 to 20 ^oC during the consecutive three days and clumped isotope followed similar trend, reflecting the influence of temperature on CO_2 Δ_{47} and rapid equilibration with the leaf and surface waters. One low value observed on the second day was probably due to plumes of vehicle exhausts, also supported by the elevated level of [CO_2] and depletion in $\delta^{13}C$ and $\delta^{18}O$ (Table 4). Effect of photosynthesis on the CO_2 was also expected specifically due the collection of samples at the grass level. However, in an open system, it is difficult to assess this with limited data points.

An elevated CO_2 concentration and low $\delta^{13}C$ and $\delta^{18}O$ values indicated significant contribution of respiration and/or anthropogenic CO_2 in the forest station (Table 4) near the Academia Sinica Campus. Though the samples were collected at 10-11 AM under bright sunlight, the vegetation was so dense that little sunlight reached the ground. Probably photosynthetic activity was not very strong at the ground level in the morning hours and the dominant process was respiration. Also poor circulation of air due to presence of high heels on the three sides of the sampling spot made the site nearly isolated from the surroundings. As a result the Δ_{47} values were observed to be similar to the thermodynamic equilibrium expected at the ambient temperatures except on 11th August, 2015 (Figure 7F). This also supports our hypothesis, made in the case of greenhouse CO_2, that respired CO_2 is always in close thermodynamic equilibrium with the substrate water. On 11th August, 2015 a significantly higher Δ_{47} value was observed. The higher value was likely due to the influence of the super Typhoon 'Soudelor' which passed over Taipei during 8-10 August, 2015 causing a decrease in temperature by 3-4 ^oC and air masses mixing in a larger spatial scale.

For high mountain CO_2, the observed Δ_{47} values (Table 4) were lower than that expected at ~10 ^oC, the ambient temperature at the top of the mountain site during sampling. The Δ_{47} values were similar to that observed in the plain and over the ocean. We note that during the sampling period, the site was affected significantly by winter monsoons. HYSPLIT 24 hours back trajectory showed marine origin of air (not shown) during the sampling time. The air CO_2 on the mountain probably did not get sufficient time to isotopically equilibrate with the local surface and leaf water but showed the signature of the marine CO_2.

643 The deviations in Δ_{47} from the thermodynamic equilibrium values in different atmospheric
644 environments and processes are summarized in Figure 9. It is obvious that the urban and sub-
645 urban CO_2 deviate the most towards lower Δ_{47} values, mainly contributed by CO_2 originated
646 from high temperature combustions, i.e., vehicular emissions. The respired CO_2 are always in
647 close thermodynamic equilibrium at the ambient temperature. On the other hand, CO_2
648 affected by strong photosynthesis show significant increase in the Δ_{47} values compared to the
649 thermodynamic equilibrium values.

650

651 **5. Summary**

652 We presented a compilation of Δ_{47} analyses for car exhaust, greenhouse and air CO_2 over a
653 wide variety of interactions in tropical and sub-tropical regions including marine, coastal,
654 urban, sub-urban, forest, and high mountain environments. Near surface marine air CO_2 is in
655 close thermodynamic equilibrium with the underlying surface water at the sea surface
656 temperature. Car exhaust, urban, sub-urban and greenhouse air CO_2 significantly deviate
657 from the thermodynamic equilibrium values. While respired CO_2 is in thermodynamic
658 equilibrium with leaf and soil surface waters, photosynthesis significantly deviates the Δ_{47}
659 values from the thermodynamic equilibrium or more precisely increases the Δ_{47} values
660 probably due to kinetic effect associated with the diffusion of CO_2 out of leaf stomata. The
661 Δ_{47} values in urban and sub-urban air CO_2 are lower than that expected under thermodynamic
662 equilibrium at the ambient temperature. The deviation is mainly due to contributions from
663 fossil fuel emissions and to some extent due to photosynthesis especially in regions with
664 dense vegetation.

665 We showed that Δ_{47} can serve as an independent tracer for studying photosynthesis. Though
666 the deviation from equilibrium during photosynthesis is also observed in oxygen clumped
667 isotopes CO_2 and O_2 are affected and produced from different processes and sources; the
668 former is affected seriously by water (water-CO_2 isotopic exchange) while the latter is
669 derived from water. We believe the analyses of the clumped isotopes for both CO_2 and O_2 are
670 of great importance in the atmospheric carbon cycling study, providing a new angle for
671 tackling the chemistry chain in photosynthesis. More systematic study in controlled
672 environments including leaf level experiments will help to better understand the role of
673 photosynthesis on Δ_{47}.

Data availability

All the data used in the manuscript are also presented in the form of Tables.

Acknowledgement

We thank Dr. Chung-Ho Wang for providing waters with different $\delta^{18}O$, Institute of Earth Sciences, Academia Sinica for providing laboratory space, Mr. Frank Lin for helping sampling in greenhouse, Dr. Jia-Lin Wang and Dr. Chang-Feng Ou-Yang for calibrating compressed air cylinder, Mr. Hao-Wei Wei for collecting air at the campus of National Taiwan University and Mr. Wei-Kang Ho for collecting oceanic CO_2 and helping in laboratory setups. Special thanks to Prof. S. K. Bhattacharya and Dr. Sasadhar Mahata for helpful discussion. This work is supported by the Ministry of Science and Technology (MOST-Taiwan) grants 105-2111-M-001-006-MY3 to Academia Sinica and 105-2119-M-002-001- to National Taiwan University.

688 **References**

689 Affek H. P., and Eiler J. M.: Abundance of mass 47 CO_2 in urban air, car exhaust, and human
690 breath, Geochim. Cosmochim. Acta, 70, 1–12, 2006.
691 Affek H. P., Xu X., and Eiler J. M.: Seasonal and diurnal variations of $^{13}C^{18}O^{16}O$ in air:
692 Initial observations from Pasadena CA, Geochim. Cosmochim. Acta**,** 71, 5033–5043,
693 2007.
694 Affek H. P., and Yakir D.: The stable isotopic composition of atmospheric CO_2, Treaties of
695 Geochemistry, 5, 179-212, 2014.
696 Affek, H. P.: Clumped isotopic equilibrium and the rate of isotope exchange between CO_2
697 and water, Am. J. Sci. 313 (4), 309–325, 2013.
698 Barkan E., and Luz B.: High precision measurements of $^{17}O/^{16}O$ and $^{18}O/^{16}O$ ratios in H_2O,
699 Rapid Commun. Mass Spectrom., 19, 3737–3742, 2005.
700 Brenninkmeijer, C. A. M., Kraft, P and Mook, W. G.: Oxygen isotope fractionation between
701 CO_2 and H_2O, Isot. Geosci., 1, 181-190, 1983.
702 Boutton, T. W.: Stable carbon isotope ratios of natural materials. II. Atmospheric, terrestrial,
703 marine, and freshwater environments, in Carbon Isotope Techniques, edited by D. C.
704 Coleman and B. Fry, pp. 173-185, Academic Press, New York, 1991.
705 Bowling, D. R., Ballantyne, A. P., Miller, J. B., Burns, S. P., Conway, T. J., Menzer, O.,
706 Stephens, B. B., and Vaughn, B. H.: Ecological processes dominate the ^{13}C land
707 disequilibrium in a Rocky Mountain subalpine forest, Global Biogeochem. Cycles, 27,
708 doi:10.1002/2013GB004686, 2014.
709 Cernusak, L. A., Farquhar, G. D., Wong, S. C., and Williams, H. S.: Measurement and
710 Interpretation of the Oxygen Isotope Composition of Carbon Dioxide Respired by
711 Leaves in the Dark, Plant Physiology, 136, 3350–3363, 2004.
712 Ciais, P., Denning, A. S., Tans, P. P., Berry, J. A., Randall, D. A., Collatz, G. J., Sellers, P.
713 J., White, J. W. C., Trolier, M., Meijer, H. A. J., Francey, R. J., Monfray, P., and
714 Heimann, M.: A three-dimensional synthesis study of $\delta^{18}O$ in atmospheric CO_2. 1.
715 Surface fluxes, J. Geophys. Res. -Atm., 102, 5857–5872, 1997.
716 Ciais, P., Tans, P. P., Trolier, M., White, J. W. C., and Francey, R. J.: A large northern-
717 hemisphere terrestrial CO_2 sink indicated by the $^{13}C/^{12}C$ ratio of atmospheric CO_2,
718 Science, 269, 1098–1102, 1995a.

719 Ciais, P., Tans, P. P., White, J. W. C., Trolier, M., Francey, R. J., Berry, J. A., Randall, D.
720 R., Sellers, P. J., Collatz, J. G., and Schimel, D. S.: Partitioning of ocean and land
721 uptake of CO_2 as inferred by $\delta^{18}O$ measurements from the NOAA Climate Monitoring
722 and Diagnostics Laboratory Global Air Sampling Network, J. Geophys. Res., 100,
723 5051–5070, 1995b.
724 Clog, M., Stolper, D., and Eiler, J. M.: Kinetics of CO2(g)–H2O(1) isotopic exchange,
725 including mass 47 isotopologues, Chem. Geol., 395, 1-10, 2015.
726 Cuntz, M., Ciais, P., Hoffmann, G., Allison, C. E., Francey, R. J., Knorr, W., Tans, P. P.,
727 White, J. W. C., and Levin, I.: A comprehensive global three-dimensional model of
728 $\delta^{18}O$ in atmospheric CO_2: 2. Mapping the atmospheric signal, J. Geophys. Res., 108,
729 (D17), DOI: 10.1029/2002jd003153, 2003.
730 Deines, P.: The isotopic composition of reduced organic carbon, in: Handbook of
731 Environmental Isotope Geochemistry, 1. The Terrestrial Environment, edited by Fritz,
732 P. and Fontes, J. C. Elsevier, 329-406, 1980.
733 Dennis, K. J., Affek, H. P., Passey, B. H., Schrag, D. P., and Eiler, J. M.: Defining an
734 absolute reference frame for 'clumped'isotope studies of CO_2, Geochim. Cosmochim.
735 Acta, 75, 7117–7131, 2011.
736 Drake, J. E., et al.: Increases in the flux of carbon belowground stimulate nitrogen uptake and
737 sustain the long-term enhancement of forest productivity under elevated CO_2, Ecology
738 Letters, 14, 349–357, 2011.
739 Eiler, J. M. and Schauble, E.: $^{18}O^{13}C^{16}O$ in Earth's atmosphere, Geochim. Cosmochim. Acta,
740 68, 4767–4777, 2004.
741 Farquhar, G. D., Ehleringer, J. R., and Hubick, K. T.: Carbon isotope discrimination and
742 photosynthesis, Annu. Rev. Plant. Physiol. Plant Mol. Biol., 40, 503-537, 1989.
743 Farquhar, G. D. and Lloyd, J.: Carbon and oxygen isotope effects in the exchange of carbon
744 dioxide between plants and the atmosphere, in: Stable isotopes and plant carbon-water
745 relations, edited by J. R. Ehleringer, A. E. Hall, and G. D. Farquhar, Academic Press,
746 New York, 47–70, 1993.
747 Farrauto, R. J.; Heck, R. M. Catalytic converters: state of the art and perspectives. Catalysis
748 Today**,** *51*, 351-360, 1999.
749 Flanagan, L. B., Brooks, J. R., Varney, G. T., Ehleringer, J. R.: Discrimination against
750 $C^{18}O^{16}O$ during photosynthesis and the oxygen isotope ratio of respired CO_2 in boreal
751 forest ecosystems, Global Biogeochem. Cycles, 11(1), 83-98, 1997.

752 Francey, R. J. and Tans, P. P.: Latitudinal variation in O-18 of atmospheric CO_2, Nature, 327,
753 495–497, 1987.
754 Francey, R. J., Tans, P. P., Allison, C. E., Enting, I. G., White, J. W. C. and Trolier, M.:
755 Changes in oceanic and terrestrial carbon uptake since 1982, Nature, 373 (6512), 326–
756 330, 1995.
757 Francois, R., Altabet, M. A., Goericke, R., McCorckle, D. C., Brunet, C., and Poisson, A.:
758 Changes in the $\delta^{13}C$ of surface water particulate organic matter across the subtropical
759 convergence in the SW Indian Ocean, Global Biogeochem. Cycles, 7(3), 627-644,
760 1993.
761 Ghosh, P., Adkins, J., Affek, H. P., Balta, B., Guo, W., Schauble, E., Schrag, D., and Eiler, J.
762 M.: $^{13}C–^{18}O$ bonds in carbonate minerals: a new kind of paleothermometer, Geochim.
763 Cosmochim. Acta, 70, 1439–1456, 2006.
764 Gillon, J., Yakir, D.: Influence of carbonic anhydrase activity in terrestrial vegetation on
765 the ^{18}O content of atmospheric CO_2, Science 291, 2584–2587, 2001.
766 Goericke, R. and Fry, B.: Variations of marine plankton $\delta^{13}C$ with latitude, temperature, and
767 dissolved CO_2 in the world ocean, Global Biogeochem. Cycles, 8(1), 85-90, 1994.
768 Hoag, K. J., Still, C. J., Fung, I. Y., and Boering, K. A.: Triple oxygen isotope composition of
769 tropospheric carbon dioxide as a tracer of terrestrial gross carbon fluxes, Geophys.
770 Res. Lett., 32, L02802, doi:10.1029/2004GL021011, 2005.
771 Hofmann, M. E. G., Horváth, B., and Pack, A.: Triple oxygen isotope equilibrium
772 fractionation between carbon dioxide and water, Earth Planet. Sci. Lett., 319–320,
773 159–164, 2012.
774 Ito, A.: A global-scale simulation of the CO_2 exchange between the atmosphere and the
775 terrestrial biosphere with a mechanistic model including stable carbon isotopes, 1953–
776 1999, Tellus 55B, 596–612, 2003.
777 Kašpar, J.; Fornasiero, P.: Hickey, N. Automotive catalytic converters: current status and
778 some perspectives, Catalysis Today, *77*, 419–449, 2003.
779 Klingstedt, F.; Arve, K.; Eränen, K.: Murzin, D. Y. Toward Improved Catalytic Low-
780 Temperature NOx Removal in Diesel-Powered Vehicles, Acc. Chem. Res., *39*, 273-
781 282, 2006.
782 Kroopnick, P., and Craig, H.: Atmospheric oxygen – Isotopic composition and solubility
783 fraction, Science, 175, 54-55, 1972.

784 Laskar, A. H., Huang, J. C., Hsu, S. C., Bhattacharya, S. K., Wang, C. H., and Liang, M. C.:
785 Stable isotopic composition of near surface atmospheric water vapor and rain–vapor
786 interaction in Taipei, Taiwan, J. Hydrol, 519, 2091-2100, 2014.
787 Laskar, A. H., Mahata, S. and Liang, M. C.: Identification of anthropogenic CO_2 using triple
788 oxygen and clumped isotpes. Environmental Science and Technology (under review),
789 2016a.
790 Liang, M. C., and Mahata. S.: Oxygen anomaly in near surface carbon dioxide reveals deep
791 stratospheric intrusion, Scientific Reports, 5, 11352, 2015.
792 Laskar, A. H., Yui, T. F. and Liang, M. C.: Clumped Isotope Composition of Marbles from
793 the Backbone Range of Taiwan. Terra Nova. DOI: 10.1111/ter.12217, 2016b.
794 Mahata, S., Bhattacharya, S. K., Wang, C. H., and Liang, M. C.: An improved CeO_2 method
795 for high-precision measurements of $^{17}O/^{16}O$ ratios for atmospheric carbon dioxide,
796 Rapid Commun. Mass Spectrom., 26, 1909−1922, 2012.
797 Miller, J. B., Lehman, S. J., Montzka, S. A., et al.: Linking emissions of fossil fuel CO_2 and
798 other anthropogenic trace gases using atmospheric $^{14}CO_2$, J. Geophys. Res., 117,
799 D08302, doi:10.1029/2011JD017048, 2012.
800 Mook, W. G.: ^{13}C in atmospheric CO_2, Neth. J. Sea Res., 20, 211-23, 1986.
801 Murayama, S., Takamura, C., Yamamoto, S., Saigusa, N., Morimoto, S., Kondo, H.,
802 Nakazawa, T., Aoki, S., Usami, T., and Kondo, M.: Seasonal variations of atmospheric
803 CO_2, $\delta^{13}C$, and $\delta^{18}O$ at a cool temperate deciduous forest in Japan: Influence of Asian
804 monsoon, J. Geophys. Res., 115, D17304, doi:10.1029/2009JD013626, 2010.
805 Newman, S., Xu, X., Affek, H. P., Stolper, E., Epstein, S.: Changes in mixing ratio and
806 isotopic composition of CO_2 in urban air from the Los Angeles basin, California,
807 between 1972 and 2003, J. Geophys. Res., 113, D23304, doi:10.1029/2008JD009999,
808 2008.
809 Pataki, D. E., Ehleringer, J. R., Flanagan, L. B., Yakir, D., Bowling, D. R., Still, C. J.,
810 Buchmann, N., Kaplan, J. O., and Berry, J. A.: The application and interpretation of
811 Keeling plots in terrestrial carbon cycle research, Global Biogeochem. Cycles,
812 17(1),1022, doi:10.1029/2001GB001850, 2003.
813 Popa, M. E., Vollmer, M. K., Jordan, A., Brand, W. A., Pathirana, S. L., Rothe, M.,
814 Röckmann, T.: Vehicle emissions of greenhouse gases and related tracers from a
815 tunnel study: $CO:CO_2$, $N_2O:CO_2$, $CH_4:CO_2$, $O_2:CO_2$ ratios, and the stable isotopes ^{13}C
816 and ^{18}O in CO_2 and CO, Atmos. Chem. Phys., 14, 2105–2123, 2014.

817 Peltier, G., Cournac, L., Despax, V., Dimon, B., Fina, L., Genty, B., and Rumeau, D.:
818 Carbonic anhydrase activity in leaves as measured in vivo by ^{18}O exchange between
819 carbon dioxide and water, Planta, 196**,** 732-739, 1995.
820 Peng, T., Wang, H. C., and Huang, C.: Stable isotopic characteristic of Taiwan's
821 precipitation: a case study of western Pacific monsoon region, Earth Planet. Sci. Lett.,
822 289 (3–4), 357–366, 2010.
823 Peylin, P., Ciais, P., Denning, A. S., Tans, P. P., Berry, J. A., and White, J. W. C.: A 3-
824 dimensional study of $\delta^{18}O$ in atmospheric CO_2: contribution of different land
825 ecosystems, Tellus Series B—Chemical and Physical Meteorology, 51(3), 642–667,
826 1999.
827 Riley, W. J., Still, C. J., Helliker, B. R., Ribas-Carbo, M., and Berry, J. A.: ^{18}O composition
828 of CO_2 and H_2O ecosystem pools and fluxes in a tallgrass prairie: simulations and
829 comparisons to measurements Global Change Biol., 9, 1567–1581, 2003.
830 Tans, P. P.,Berry, J. A., and Keeling, R. F.: Oceanic $^{13}C/^{12}C$ observations: A new window on
831 ocean CO_2 uptake, Global Biogeochim. Cycles, 7(2) 353–368, 1993.
832 Thiemens, M. H., Chakraborty, S., Jackson, T. L.: Decadal $\Delta^{17}O$ record of tropospheric CO_2:
833 Verification of a stratospheric component in the troposphere, J. Geophys. Res., 119,
834 6221–6229, 2014.
835 Wang, Z., Schauble, E. A., and Eiler, J. M.: Equilibrium thermodynamics of multiply
836 substituted isotopologues of molecular gases, Geochim. Cosmochim. Acta, 68(23),
837 4779–4797, 2004.
838 Welp, L. R., Keeling, R. F., Meijer, H. A. J., Bollenbacher, A. F., Piper, S. C., Yoshimura,
839 K., Francey, R. J., Allison, C. E., and Wahlen, M.: Interannual variability in the
840 oxygen isotopes of atmospheric CO_2 driven by El Nino, Nature, 477, 579-582, 2011.
841 Yakir, D., and Wang, X. F.: Fluxes of CO_2 and water between terrestrial vegetation and the
842 atmosphere estimated from isotope measurements, Nature, 380, 515-517, 1996.
843 Ye, F., Deng, W., Xie, L., Wei, G., and Jia, G.: Surface water $\delta^{18}O$ in the marginal China seas
844 and its hydrological implications. Estuarine, Coastal and Shelf Science 147, 25-31,
845 2014.
846 Yeung, L. Y. et al.: Large and unexpected enrichment in stratospheric $^{16}O^{13}C^{18}O$ and its
847 meredional variation, Proc. Nat. Acad. Sci. USA, 106(28), 11496-11501, 2009.
848 Yeung, L. Y., Ash, J. L., and Young, E. D.: Biological signatures in clumped isotopes of O_2,
849 Science 348, 431–434, 2015.

Zhai, W., Dai, M., Cai,W. J., Wang, Y., and Hong, H.: The partial pressure of carbon dioxide and air-sea fluxes in the northern South China Sea in spring, summer and autum., Mar. Chem., 96, 87–97, 2005.

Zhang, J., P. Quay, D., and Wilbur, D. O.: Carbon isotope fractionation during gas-water exchange and dissolution of CO_2, Geochim. Cosmochim. Acta., doi:10.1016/0016-7037(95)91550-d, 1995.

Figures

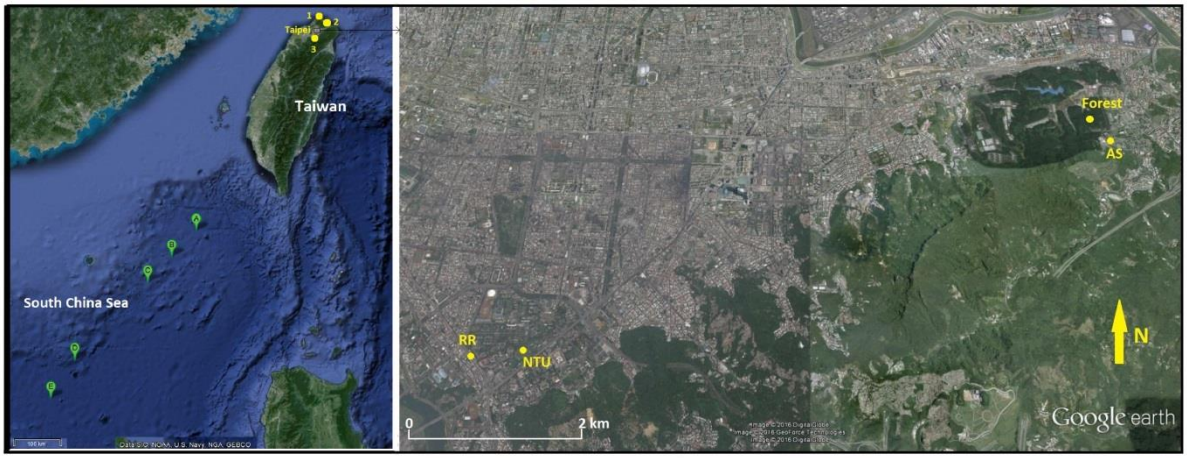

Figure 1. Left panel: map of Taiwan and South China Sea with the locations marine air sampling stations (A to E). The coastal stations 1 and 2 are Fuguei Cape and Keelung and 3 is the high mountain station Hehuan (~3.2 km a.s.l.). Right panel: Part of Taipei city with sampling stations Roosevelt Road (RR), grassland in the National Taiwan University (NTU) Campus, sub-urban site inside the campus of Academia Sinica (AS) and forest site.

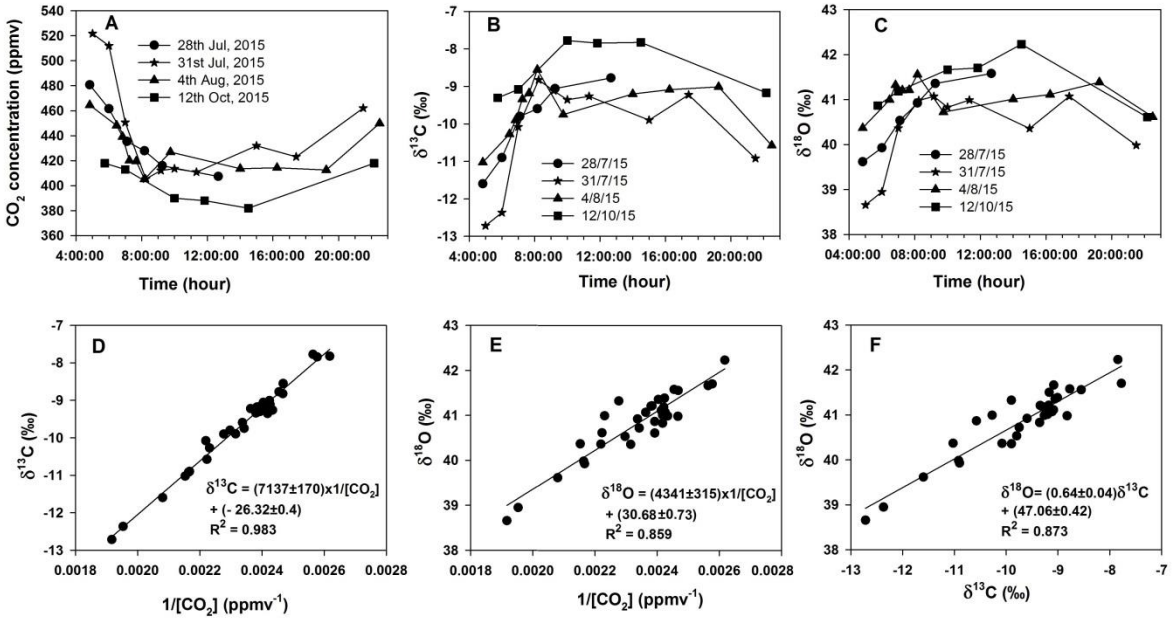

Figure 2. Top panels show the diurnal variation of (A) concentration, (B) $\delta^{13}C$, and (C) $\delta^{18}O$ of CO_2 sampled in the greenhouse. Bottom panels are the Keeling plots for (D) $\delta^{13}C$ and (E) $\delta^{18}O$ and (F) scatter plot of $\delta^{13}C$ and $\delta^{18}O$ to show their covariance.

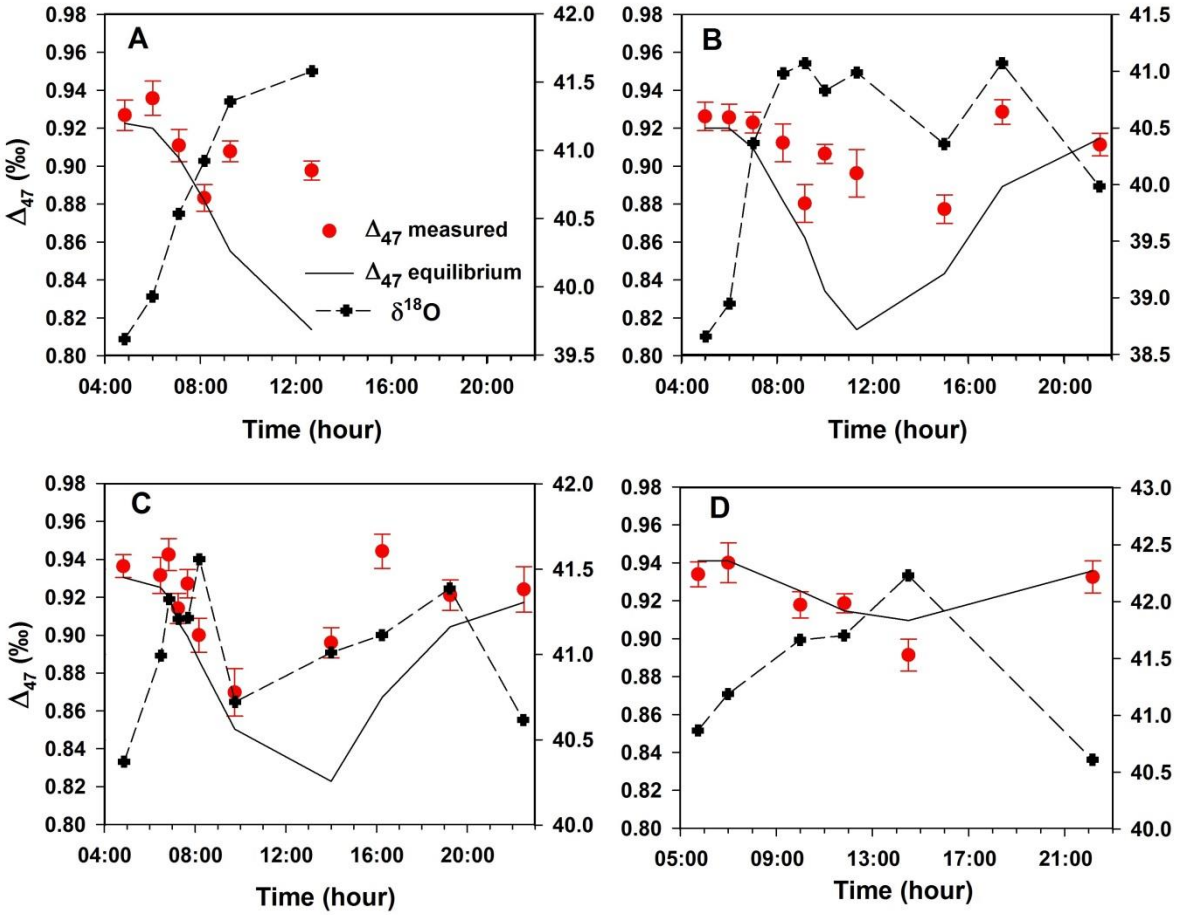

Figure 3. Diurnal variation of the Δ_{47} and $\delta^{18}O$ values in the greenhouse for samples collected on four days of 2015: (A) 28th July, (B) 31st July, (C) 4th August, and (D) 12th October. The first three days (A-C) were bright sunny days and the last one (D) a cloudy day with covered rooftop (see texts for details). The error bars are 1 standard error associated with the measurements.

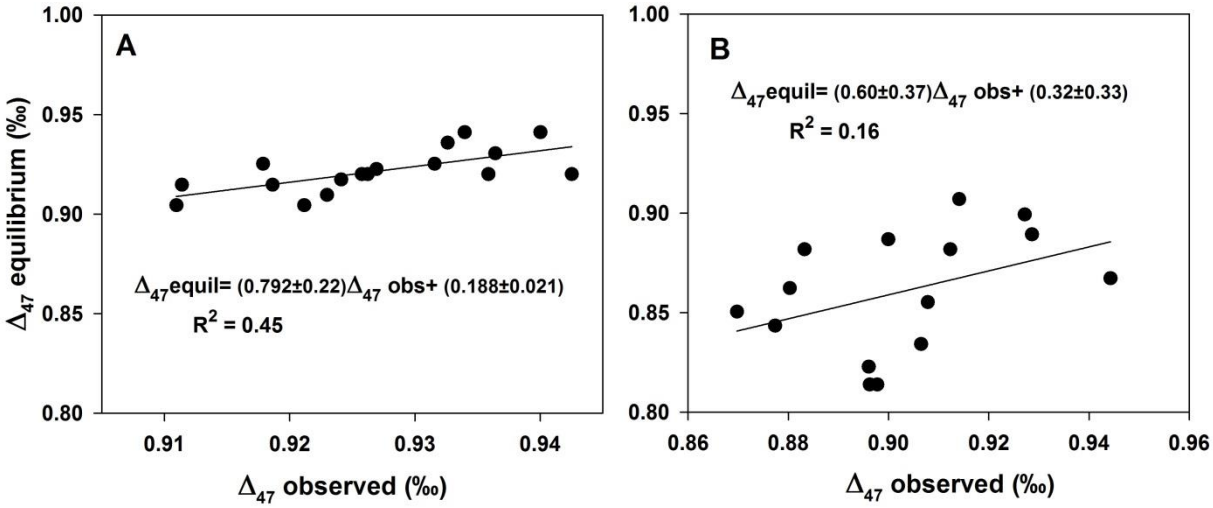

Figure 4. Correlation between the observed and thermodynamic equilibrium Δ_{47} values for greenhouse CO_2 samples collected when (A) photosynthesis ass weak and respiration was strong and (B) photosynthesis was strong and respiration was weak.

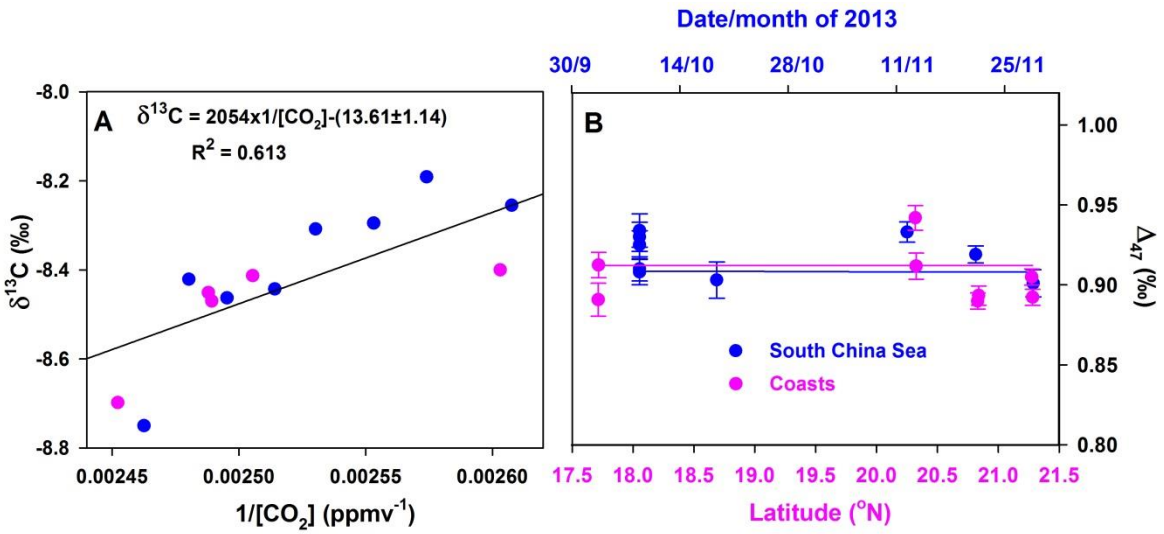

Figure 5. (A) Carbon Keeling plot for air CO_2 collected over South China Sea and coastal stations (Keelung and Fuguei Cape). (B) Δ_{47} values observed over the South China Sea and coastal stations. The error bars are the 1 standard error associated with the measurements. Lines show Δ_{47} values for the CO_2 in thermodynamic equilibrium at ambient temperatures.

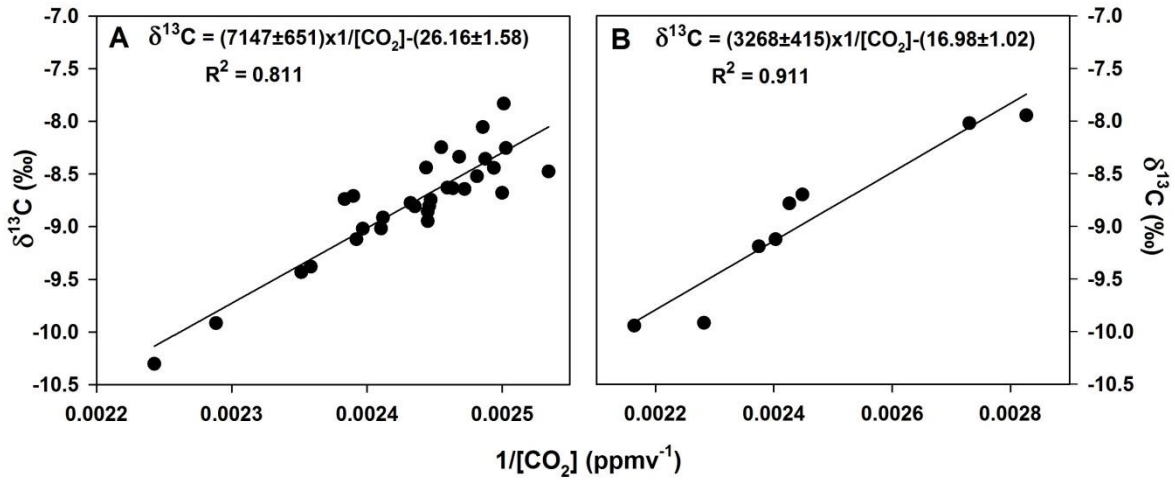

Figure 6. Carbon Keeling plots for air CO_2 collected over (A) sub-urban Academia Sinica Campus and (B) grassland at National Taiwan University Campus.

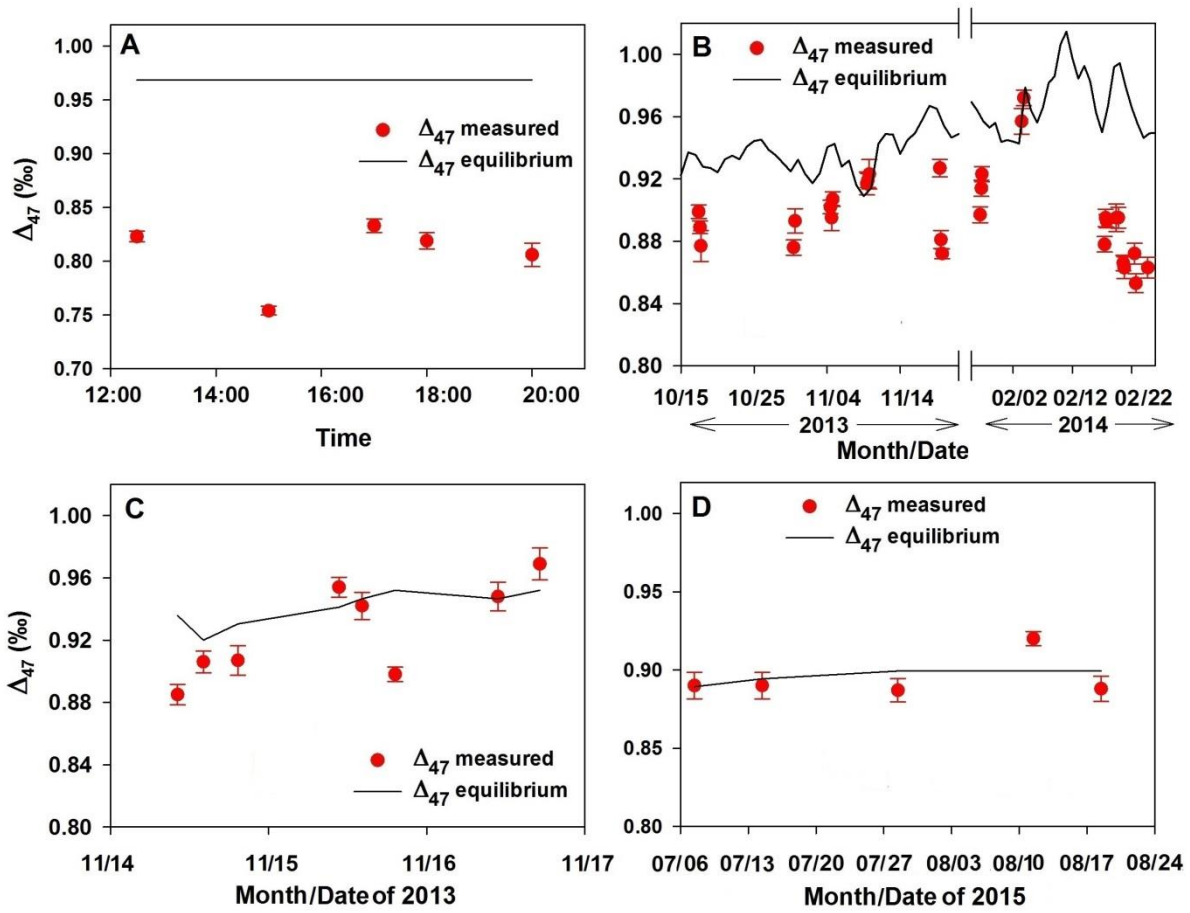

925

926 Figure 7. Δ_{47} values in the near surface atmospheric CO_2 from (A) urban site near Roosevelt
927 Road on 30th December, 2015, (B) sub-urban station (Academia Sinica Campus), (C)
928 grassland in the National Taiwan University Campus and (D) forest site near the Academia
929 Sinica Campus. The error bars are the 1 standard error associated with the measurements.
930 Lines show Δ_{47} values for the CO_2 at thermodynamic equilibrium at ambient temperatures.

931

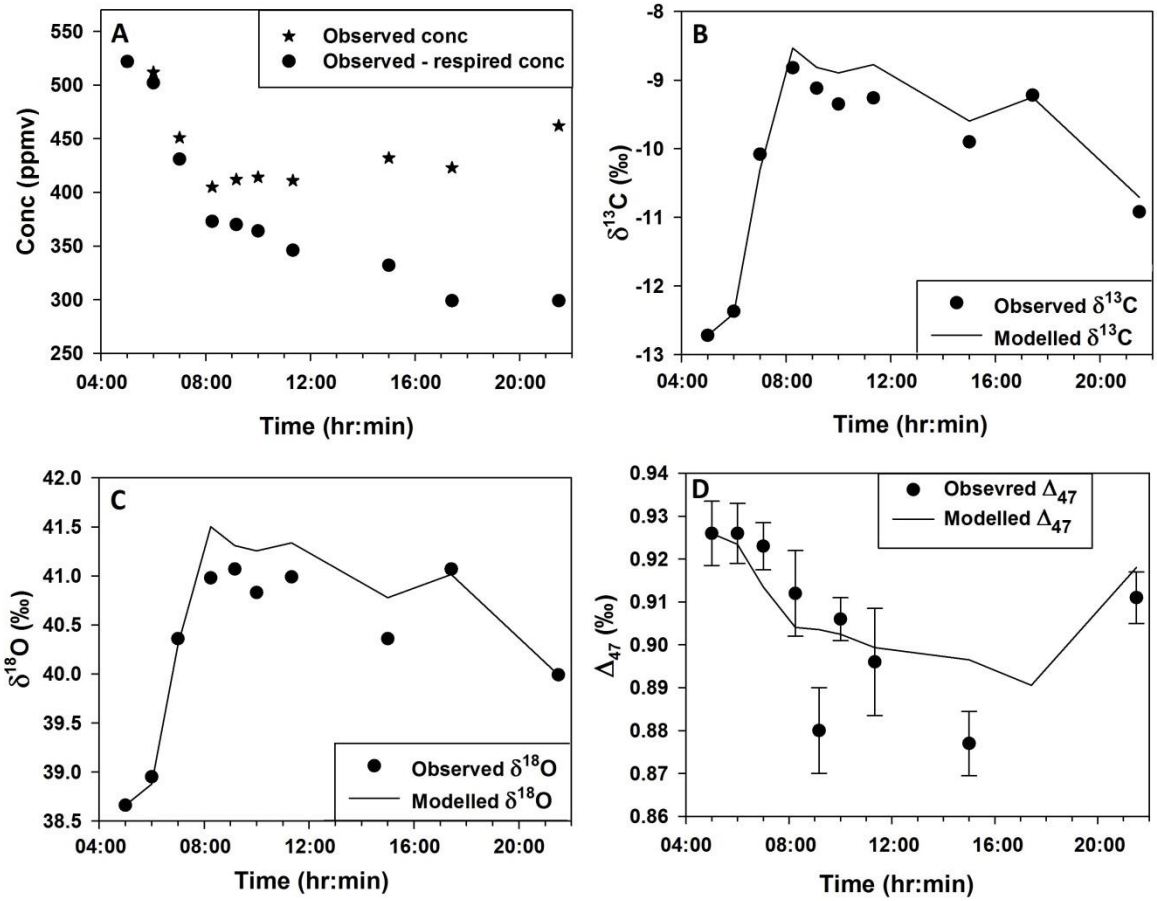

Figure 8: (A) CO_2 concentration inside greenhouse on 31st Aug, 2015: observed concentration (star) and decrease in concentration by photosynthesis after subtracting the respiration (solid circle) are also shown. Comparison of observed (B) $\delta^{13}C$, (C) $\delta^{18}O$ and (D) Δ_{47} values with that modelled using discrimination factors of -16.5 ‰, -11.2 ‰ and 0.065 ‰ for $\delta^{13}C$, $\delta^{18}O$ and Δ_{47} respectively.

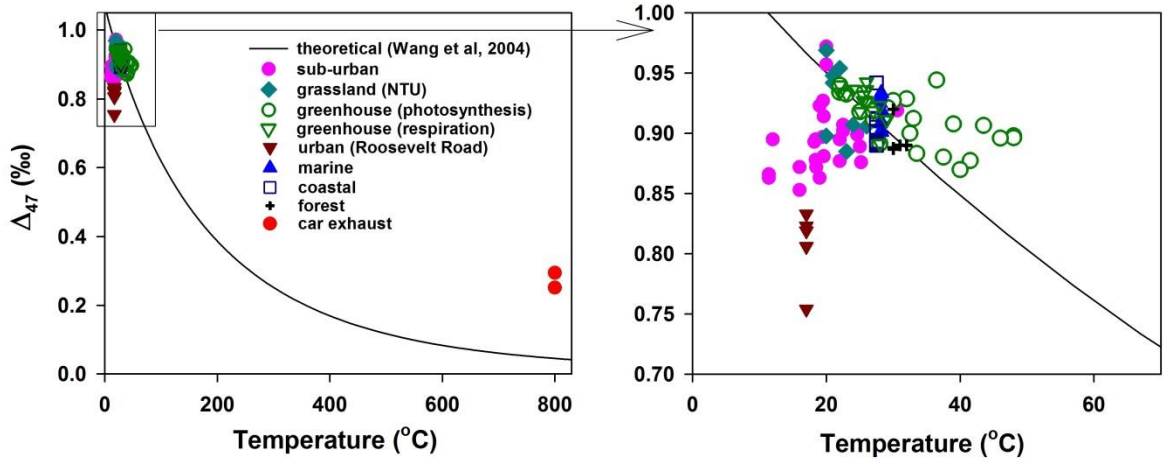

Figure 9. A summary of Δ_{47} values in near surface air CO_2 obtained at different environments and compared with the thermodynamic equilibrium values. Combustion temperature for car exhausts is assumed to be 800 ^{o}C (minimum value). Greenhouse CO_2 are divided into two categories: photosynthesis dominated (green open circle) and respiration dominated (green open triangle).

965 Table 1. Diurnal variation of $\delta^{13}C$ and $\delta^{18}O$ and clumped isotopes (Δ_{47}) for greenhouse CO_2. Temperatures estimated using Δ_{47} values and actual air
966 temperatures inside the greenhouse at the time of sampling are also presented.
967

Date	Time	Conc. (ppmv)	$\delta^{13}C$(‰) (VPDB)	$\delta^{18}O$(‰) (VSMOW)	δ^{47}(‰)	Std. err.	Δ_{47} (‰) (ARF)	Std. err.	Δ_{48} (‰)	Estimated temp. (^{o}C)	Air temp. (^{o}C)
7/28/2015	4:50	481	-11.60	39.61	6.99	0.02	0.927	0.016	0.2	24	25.5
	6:00	462	-10.90	39.92	8.16	0.02	0.936	0.018	0.6	21	26
	7:06	435	-9.80	40.54	9.71	0.02	0.911	0.017	0.2	28	29
	8:10	428	-9.60	40.92	10.38	0.02	0.883	0.014	-0.2	33	33.5
	9:15	416	-9.06	41.36	11.30	0.01	0.908	0.011	0.2	24	39
	10:15	422	-9.55	40.82	NA	NA	NA	NA	NA	NA	NA
	12:40	407	-8.77	41.58	11.75	0.01	0.898	0.010	0.2	27	48
7/31/2015	5:00	522	-12.72	38.66	5.10	0.01	0.926	0.015	0.3	24	26
	6:00	512	-12.37	38.95	5.94	0.01	0.926	0.014	0.5	25	26
	7:00	451	-10.08	40.36	9.39	0.02	0.923	0.011	0.4	25	28
	8:15	405	-8.82	40.98	11.25	0.02	0.912	0.020	0.4	28	33
	9:10	412	-9.12	41.07	11.26	0.02	0.880	0.020	0.6	34	37.5
	10:00	414	-9.35	40.83	11.52	0.01	0.906	0.010	0.6	23	43.5
	11:20	411	-9.26	40.99	11.12	0.02	0.896	0.025	0.5	31	48
	15:00	432	-9.90	40.36	9.55	0.02	0.877	0.015	0.5	34	41.5
	17:25	423	-9.22	41.07	12.48	0.02	0.929	0.013	0.7	25	32
	21:30	462	-10.92	39.99	7.90	0.01	0.911	0.012	0.4	28	27
8/4/2015	4:50	465	-11.03	40.37	8.41	0.01	0.936	0.012	0.27	23	24
	5:50	455	-10.82	40.26	NA	NA	NA	NA	NA	NA	NA
	6:28	448	-10.27	41.00	10.01	0.02	0.931	0.017	0.7	24	25.5
	6:50	439	-9.90	41.32	10.10	0.02	0.942	0.009	0.6	22	26

	7:15	420	-9.34	41.22	11.05	0.01	0.914	0.013	0.6	28	28.5
	7:40	419	-9.18	41.22	11.05	0.01	0.927	0.011	0.3	25	30
	8:10	405	-8.55	41.56	12.79	0.02	0.900	0.015	0.6	31	32.5
	9:45	427	-9.75	40.73	10.81	0.02	0.870	0.023	0.3	36	40
	14:00	414	-9.20	41.01	11.02	0.01	0.896	0.011	0.6	31	46
	16:15	414	-9.09	41.11	11.11	0.01	0.944	0.014	0.7	22	36.5
	19:15	413	-9.01	41.38	13.28	0.01	0.921	0.010	0.9	26	29.2
	22:30	450	-10.58	40.61	9.34	0.02	0.924	0.022	0.4	25	26.5
10/12/2015	5:45	418	-9.30	40.87	10.80	0.01	0.934	0.013	0.5	23	22
	7:00	413	-9.08	41.18	10.95	0.02	0.940	0.021	0.4	22	22
	10:00	390	-7.78	41.66	13.00	0.02	0.918	0.014	0.6	26	25
	11:50	388	-7.84	41.71	15.25	0.01	0.919	0.010	0.6	26	27
	14:30	382	-7.82	42.24	14.27	0.02	0.891	0.017	0.4	31	28
	20:10	418	-9.17	40.61	10.85	0.02	0.933	0.017	0.5	23	23

Table 2. Stable carbon and oxygen isotopic composition and clumped isotopes (Δ_{47}) for car exhaust CO_2. Temperatures estimated using Δ_{47} values and lowest possible combustion temperatures are given.

Car model	Conc. (ppm)	$\delta^{13}C$(‰) (VPDB)	$\delta^{18}O$(‰) (VSMOW)	δ^{47}(‰)	Std. err.	Δ_{47} (‰) (ARF)	Std. err.	Δ_{48} (‰)	Estimated temp. (^{o}C)	Combustion temp. (^{o}C)
Mazda 3000cc TRIBUTE	39400	-27.73	25.43	-22.20	0.01	0.251	0.013	-0.4	300	800
Mitsubishi 2400cc New Outlander	39300	-27.67	25.27	-23.08	0.02	0.294	0.007	-0.3	265	800
Average ± 1σ	39350±50	-27.70±0.03	25.35±0.07	-22.64±0.44		0.273±0.021			283±18	

Table 3. Stable isotopic composition including Δ_{47} for air CO_2 collected over South China Sea and two coastal stations (see Figure 1 for sampling locations). Temperatures estimated using Δ_{47} values and the sea surface temperatures at the time of samplings are also presented.

Marine air CO_2										
South China Sea										
Date time	Conc. (ppm)	$\delta^{13}C$(‰) (VPDB)	$\delta^{18}O$(‰) (VSMOW)	δ^{47}(‰)	Std. err.	Δ_{47} (‰) (ARF)	Std. err.	Δ_{48} (‰)	Estimated temp. (^oC)	Sea surface temp. (^oC)
10/15/2013 8:15 (A)*	403	-8.42	40.85	28.752	0.016	0.901	0.017	1.9	30	28.3
10/15/2013 13:15 (B)	400	-8.46	40.80	28.441	0.012	0.919	0.011	2.6	26	28.3
10/15/2013 18:00 (C)	406	-8.75	40.54	28.133	0.013	0.933	0.013	2.2	24	28.3
10/16/2013 7:00 (D)	391	-8.76	40.53	27.916	0.024	0.903	0.023	3.9	29	28.2
10/16/2013 12:05 (E)	397	-8.44	40.86	28.535	0.015	0.910	0.015	3.3	28	28.2
10/16/2013 14:00 (E)	391	-8.30	40.96	28.922	0.021	0.934	0.021	3.0	23	28.2
10/16/2013 17:20 (E)	395	-8.31	41.02	28.944	0.017	0.908	0.016	1.9	29	28.1
10/16/2013 20:20 (E)	388	-8.19	40.52	28.909	0.018	0.930	0.018	3.8	24	28.1
10/17/2013 8:40 (E)	383	-8.26	40.41	28.194	0.018	0.925	0.018	4.3	25	28.1
Average ± 1σ	395±7	-8.43±0.19	40.72±0.20	28.52±0.36		0.918±0.012			27±2	28.2±0.1
Keelung										
10/03/2013 11:30	380	-8.31	40.31	28.053	0.020	0.896	0.021	3	31	27.5
10/03/2013 12:30	384	-8.40	40.92	29.089	0.017	0.917	0.016	1.9	27	27.5

11/13/2013 11:00	401	-8.45	40.62	29.645	0.015	0.946	0.016	4.0	21	27.5
11/21/2013 12:30		-8.47	40.78	29.866	0.017	0.890	0.010	1.1	32	27.5
11/28/2013 12:00	410	-8.60	40.21	28.992	0.011	0.908	0.010	2.2	28	27.5
Average ± 1σ	394±12	-8.45±0.09	40.57±0.26	29.12±0.63		0.911±0.020			28±4	27.5
Fuguei Cape										
11/13/2013 13:30	401	-8.47	40.76	29.56	0.02	0.916	0.016	1.1	27	27.5
11/21/2013 15:30	399	-8.41	40.89	29.37	0.01	0.880	0.012	2.5	34	27.5
11/28/2013 15:00	407	-8.70	41.16	30.11	0.01	0.886	0.010	3.1	33	27.5
Average ± 1σ	402±3	-8.53±0.12	40.94±0.16	29.68±0.29		0.894±0.015			31±3	27.5

*Sampling Stations (see Figure 1 for locations in South China Sea)

Table 4. Stable isotopic composition including clumped isotopes (Δ_{47}) for air CO_2 collected in urban and sub-urban stations, grassland, forest and high mountain environments. Temperatures estimated using Δ_{47} values and air temperatures are also presented.

Urban CO_2: Roosevelt Road, Taipei City											
Date	Time	Conc. (ppm)	$\delta^{13}C$(‰) (VPDB)	$\delta^{18}O$(‰) (VSMOW)	δ^{47}(‰)	Std. err.	Δ_{47} (‰) (ARF)	Std. err.	Δ_{48} (‰)	Estimated temp. (^oC)	Air temp. (^oC)
12/30/ 2015	12:30	510	-10.41	40.00	25.26	0.014	0.823	0.010	2.3	46	20
	15:00	478	-11.50	38.49	22.63	0.012	0.754	0.008	0.9	62	19.5
	17:00	461	-9.69	40.70	26.74	0.017	0.833	0.013	0.9	44	17
	18:00	594	-12.30	38.14	21.56	0.014	0.819	0.015	1.5	47	16
	20:00	457	-11.34	39.24	23.61	0.022	0.806	0.022	3.1	50	15
Average±1σ		500±50	-11.05±0.90	39.31±0.94	23.96±1.84		0.807±0.028			50±6	17±2

Sub-urban air CO_2										
Academia Sinica Campus										
Date time	Conc. (ppm)	$\delta^{13}C$(‰) (VPDB)	$\delta^{18}O$(‰) (VSMOW)	δ^{47}(‰)	Std. err.	Δ_{47} (‰) (ARF)	Std. err.	Δ_{48} (‰)	Estimated temp. (^{o}C)	Air temp (^{o}C)
10/17/2013 10:00	400	-7.83	40.44	28.47	0.015	0.899	0.008	3.7	30	25
10/17/2013 14:30	402	-8.05	40.25	28.07	0.017	0.889	0.008	2.2	32	25
10/17/2013 17:20	409	-8.44	39.90	27.26	0.019	0.877	0.020	2.3	34	22
10/30/2013 10:00	395	-8.48	40.57	28.47	0.012	0.876	0.010	2.8	35	25.2
10/30/2013 14:30	400	-8.25	41.08	29.03	0.016	0.893	0.016	3.9	31	27.4
11/04/2013 10:30	411	-8.78	40.51	28.67	0.011	0.902	0.009	2.7	29	22.5
11/04/2013 14:30	406	-8.64	40.62	28.97	0.017	0.895	0.016	2.2	31	22
11/04/2013 18:30	415	-9.02	40.38	28.33	0.013	0.907	0.009	2.8	28	22.5
11/09/2013 10:30	405	-8.34	41.09	29.79	0.019	0.917	0.015	1.9	27	28.5
11/09/2013 14:00	407	-8.25	41.25	30.63	0.015	0.919	0.009	1.6	26	30.6
11/09/2013 18:30	425	-9.43	40.32	27.49	0.020	0.923	0.019	2.1	25	28
11/19/2013 10:00	419	-8.74	40.60	29.27	0.012	0.927	0.011	3.7	25	19.5
11/19/2013 14:00	418	-8.71	40.52	29.59	0.019	0.881	0.012	1.2	33	19.6
11/19/2013 18:00	414	-8.91	40.56	28.58	0.012	0.872	0.006	1.1	35	18.5
01/27/2014 10:30	403	-8.52	41.32	30.13	0.008	0.897	0.010	2.9	30	19.2
01/27/2014 15:20	400	-8.68	41.23	30.03	0.011	0.914	0.010	0.7	27	19.6
01/27/2014 18:00	404	-8.64	41.32	29.29	0.017	0.923	0.010	4.6	25	18.5
02/03/2014 11:00	408	-8.80	41.20	29.67	0.015	0.957	0.017	1.7	19	24.5
02/03/2014 14:30	409	-8.86	41.39	NA		NA		NA		
02/03/2014 19:30	409	-8.95	41.41	30.57	0.011	0.972	0.010	3.0	16	19.3

02/17/2014 10:30	445	-10.30	40.40	27.60	0.016	0.878	0.010	3.0	34	22.4
02/17/2014 14:30	408	-8.74	41.53	30.58	0.014	0.895	0.011	0.6	31	25
02/17/2014 18:30	437	-9.92	41.07	28.49	0.012	0.893	0.008	1.3	31	22
02/19/2014 10:00	418	-9.12	40.61	29.12	0.020	0.895	0.018	0.9	31	13.3
02/19/2014 18:00	424	-9.38	40.40	28.49	0.020	0.895	0.013	2.4	31	12.4
02/20/2014 14:30	410	-8.81	40.96	29.68	0.023	0.866	0.010	1.9	37	12.9
02/20/2014 18:00	417	-9.02	40.66	29.59	0.018	0.863	0.014	1.6	37	12.5
02/22/2014 12:15	401	-8.44	41.49	30.63	0.013	0.872	0.013	0.6	35	17.5
02/22/2014 17:00	402	-8.36	41.51	30.63	0.013	0.853	0.012	4.2	40	17.1
02/24/2014 17:30	406	-8.63	41.57	30.70	0.014	0.863	0.013	3.8	37	22
Average ± 1σ	411±11	-8.78±0.50	40.87±0.46	29.23±1.00		0.897±0.027			30±5	21±5
Grassland: NTU Campus										
11/14/2013 10:10	353	-7.95	40.96	30.18	0.02	0.885	0.013	0.4	33	23
11/14/2013 14:05	366	-8.02	41.31	30.79	0.01	0.906	0.014	0.4	29	26
11/14/2013 19:20	462	-9.94	38.33	25.64	0.02	0.907	0.019	0.2	29	24
11/15/2013 10:40	416	-9.12	39.42	29.51	0.01	0.954	0.013	0.6	20	22
11/15/2013 14:10	421	-9.19	39.36	29.78	0.02	0.942	0.018	0.3	22	21
11/15/2013 19:12	438	-9.92	38.28	28.08	0.04	0.989	0.009	0.0	13	20
11/16/2013 10:50	412	-8.78	40.03	28.54	0.02	0.948	0.018	1.8	21	21
11/16/2013 17:10	408	-8.70	40.26	26.06	0.02	0.969	0.021	1.6	17	20
Average ± 1σ	409±33	-8.95±0.70	39.74±1.00	28.57±1.77		0.937±0.030			23±6	22±2
Forest site near Academia Sinica Campus										
07/07/2015 10:30	411	-9.07	41.43	11.54	0.01	0.890	0.017	0.3	32	32
07/14/2015 10:30	458	-10.43	39.74	9.01	0.02	0.890	0.017	0.4	32	31
07/28/2015 10:40	441	-9.99	40.86	10.07	0.02	0.887	0.015	0.2	32	30
08/11/2015 10:40	448	-10.46	40.09	9.50	0.01	0.920	0.009	0.5	26	30

08/18/2015 10:30	433	-9.99	39.80	8.99	0.02	0.888	0.016	0.4	32	30
Average ± 1σ	438±16	-9.99 ±0.50	40.39±0.66	9.82±0.94		0.895±0.012			31±2	31±1
High mountain: Hehuan										
10/09/2013 13:20	364	-8.21	40.89	28.79	0.02	0.895	0.016	3.2	31	10
10/09/2013 17:00	NA	-8.25	40.28	28.41	0.01	0.914	0.014	2.9	27	10
Average ± 1σ	364	-8.23 ±0.02	40.59±0.30	28.60±0.19		0.904±0.009			30±2	10

989